

SHARP STATISTICAL LIMITS AND ALGORITHM FOR ATTRIBUTED GRAPH ALIGNMENT

Anonymous authors

Paper under double-blind review

ABSTRACT

This paper investigates the problem of recovering hidden vertex mappings between two correlated weighted graphs with both edge structure and node features. While most existing studies on graph alignment focus solely on edge information, many practical scenarios also provide node features in addition to graph topology. To address this setting, we introduce the featured correlated Gaussian Wigner model, in which the graphs are correlated through a latent vertex permutation, and the associated features are also correlated under the same permutation. We establish the optimal information-theoretic thresholds for recovering the latent vertex mappings. Furthermore, we propose QPAlign, a fast algorithm leveraging quadratic programming relaxation to the Birkhoff polytope, and validate its effectiveness on both synthetic and real datasets.

1 INTRODUCTION

Graph alignment is a fundamental problem in network science and machine learning, with applications in many areas. For example, in computer vision, 3-D shapes can be represented as graphs and a significant problem for pattern recognition and image processing is determining whether two graphs represent the same object under rotations (Berg et al., 2005; Mateus et al., 2008); in natural language processing, each sentence can be represented as a graph and the ontology problem refers to uncovering the correlation between different knowledge graphs that are in different languages (Haghighi et al., 2005); in computational biology, proteins can be regarded as vertices and the interactions between them can be formulated as weighted edges (Singh et al., 2008; Vogelstein et al., 2015).

Since real-world scenarios often present challenges due to the noise in real data, many studies focused on random graph models to serve as a pivotal step, including graph alignment problem in Erdős-Rényi model (Wu et al., 2022; Ding & Du, 2023b; Huang et al., 2024), Gaussian Wigner model (Fan et al., 2023a; Araya et al., 2024; Ding & Li, 2024), stochastic block model (Onaran et al., 2016; Lyzinski, 2018; Chai & Rácz, 2024), and graphon model (Zhang, 2018). However, previous works on random graph alignment mainly focus on models that rely solely on topological information. In real scenarios, however, feature information often plays a crucial role. For instance, in the ACM-DBLP dataset, node features such as paper titles or author names are essential for identifying corresponding entities across the two graphs (Tang et al., 2023; Bommakanti et al., 2024). This motivates the study of alignment models that incorporate both structural and feature information, beyond purely topology-based settings.

While existing work on attributed graph alignment mostly builds on correlated Erdős-Rényi or community-based model with binary edges and node attributes (Zhang et al., 2024; Yang & Chung, 2024; 2025), many real-world networks are both weighted and attributed. For example, in gene co-expression networks (Zhang & Horvath, 2005), edge weights encode co-expression strength while genes carry functional annotations, and in social networks (Leskovec et al., 2010), edges record rating or interaction strengths while nodes have profile or content features. To bridge this gap, we investigate the following Featured correlated Gaussian Wigner model.

Definition 1 (Featured correlated Gaussian Wigner model). *Let G_1 and G_2 be two weighted random graphs with vertex sets $V(G_1), V(G_2)$ such that $|V(G_1)| = |V(G_2)| = n$. Let π^* denote a latent bijective mapping from $V(G_1)$ to $V(G_2)$. We say that a pair of graphs (G_1, G_2) follows featured correlated Gaussian Wigner model $\mathcal{G}(n, d, \rho, r)$ if*

1. each pair of weighted edges $\beta_{uv}(G_1)$ and $\beta_{\pi^*(u)\pi^*(v)}(G_2)$ for any $u, v \in V(G_1)$ are correlated standard normals with correlation coefficient $\rho \in (0, 1)$;
2. each pair of features $(\mathbf{x}_u, \mathbf{y}_{\pi^*(u)})$ for any $u \in V(G_1)$ follows multivariate normal distribution $\mathcal{N}(0, \Sigma_d)$ with $\Sigma_d = \begin{bmatrix} I_d & rI_d \\ rI_d & I_d \end{bmatrix}$, where the dimension $d \in \mathbb{N}$ and the correlation $r \in (0, 1)$. Moreover, we assume that the features are independent with the weighted edges.

We assume features are standardized so that each coordinate has unit variance and is independent, which justifies the identity matrices in Σ_d . Edge weights are likewise centered and variance-normalized, with correlations ρ and r capturing structural and feature dependence, respectively. Furthermore, we assume $\rho, r \in (0, 1)$ without loss of generality, since the model is invariant under flipping the signs of all edge weights or node features in G_2 , and hence negative correlations can be reduced to positive ones. Indeed, this model bridges two significant extremes, it reduces to correlated Gaussian Wigner model (Ding et al., 2021) when $r = 0$ and correlated Gaussian database model (Dai et al., 2019a) when $\rho = 0$. Given G_1 and G_2 under $\mathcal{G}(n, d, \rho, r)$, our goal is to recover the latent vertex mapping π^* . More specifically, given two permutations $\pi^*, \hat{\pi} : V(G_1) \mapsto V(G_2)$, denote the fraction of their overlap by $\text{overlap}(\pi^*, \hat{\pi}) = \frac{1}{n} |\{v \in V(G_1) : \pi^*(v) = \hat{\pi}(v)\}|$. To quantify the performance of an estimator $\hat{\pi}$, we say an estimator $\hat{\pi}(G_1, G_2)$ achieves

- *partial recovery*, if $\text{overlap}(\hat{\pi}, \pi^*) \geq \delta$ for some $\delta \in (0, 1)$;
- *exact recovery*, if $\text{overlap}(\hat{\pi}, \pi^*) = 1$.

1.1 MAIN RESULTS

In this subsection, we present our main results on information-theoretic thresholds. Let \mathcal{S}_n denote the set of bijective mappings $\pi : V(G_1) \mapsto V(G_2)$. Our goal is to determine the correlation required for successful recovery of π^* . Next, we introduce our main theorems.

Theorem 1 (Partial Recovery). *If $d = \omega(\log n)$ and $n \log(\frac{1}{1-\rho^2}) + 2d \log(\frac{1}{1-r^2}) \geq (4 + \epsilon) \log n$ for some constant $\epsilon > 0$, then there exists an estimator $\hat{\pi}$ such that, for any fixed constant $0 < \delta < 1$ and $\pi^* \in \mathcal{S}_n$, we have*

$$\mathbb{P}[\text{overlap}(\hat{\pi}, \pi^*) \geq \delta] = 1 - o(1).$$

Conversely, for any $0 < \delta < 1$, if $n \log(\frac{1}{1-\rho^2}) + 2d \log(\frac{1}{1-r^2}) \leq c \log n$ for some constant c , then for any estimator $\hat{\pi}$,

$$\mathbb{P}[\text{overlap}(\hat{\pi}, \pi^*) < \delta] \geq 1 - \frac{c}{4\delta},$$

where π^ is uniformly distributed over \mathcal{S}_n .*

The upper bound holds uniformly over all $\pi^* \in \mathcal{S}_n$, while the lower bound is obtained by analyzing the Bayes risk under the uniform prior on π^* , which is least favorable in our permutation-symmetric model and therefore leads to the same threshold for the minimax risk. Consequently, the threshold is valid for both minimax and Bayesian risks. As for the assumption $d = \omega(\log n)$, it is standard in Gaussian database alignment: identifying a vertex among n candidates requires $\Theta(\log n)$ bits, while each feature coordinate contributes only $O(1)$ bits of discriminative information, so the total feature dimension must eventually dominate $\log n$ (see, e.g., Dai et al. (2019a)). Theorem 1 characterizes the optimal rate for the information-theoretic threshold in the partial recovery regime. In particular, the special case $\delta = 1$ corresponds to exact recovery. For obtaining a sharper constant in this regime, we have the following theorem.

Theorem 2 (Exact Recovery). *If $d = \omega(\log n)$ and $n \log(\frac{1}{1-\rho^2}) + d \log(\frac{1}{1-r^2}) \geq (4 + \epsilon) \log n$ for some constant $\epsilon > 0$, then there exists an estimator $\hat{\pi}$ such that, for any fixed constant $0 < \delta < 1$ and $\pi^* \in \mathcal{S}_n$, we have*

$$\mathbb{P}[\text{overlap}(\hat{\pi}, \pi^*) = 1] = 1 - o(1).$$

Conversely, if $r^2 \geq \frac{40}{d}$ and $n \log(\frac{1}{1-\rho^2}) + d \log(\frac{1}{1-r^2}) + 4 \log d \leq (4 - \epsilon) \log n$ for some constant $\epsilon > 0$, then for any estimator $\hat{\pi}$,

$$\mathbb{P}[\text{overlap}(\hat{\pi}, \pi^*) \neq 1] = 1 - o(1),$$

where π^ is uniformly distributed over \mathcal{S}_n .*

The technical condition $r^2 \geq 40/d$ is only imposed to sharpen the leading constant in this regime: Theorem 1 already yields the optimal rate without this assumption under the special case $\delta = 1$, while under $d = n^{o(1)}$ and $d = \omega(\log n)$ such a lower bound on the feature signal ensures that our exact recovery threshold attains the optimal constant. In comparison with the special case $\delta = 1$ in Theorem 1, Theorem 2 establishes a sharper information-theoretic threshold for exact recovery under certain conditions on d . Indeed, the difference between the $2d$ -term in partial recovery and the d -term in exact recovery arises because exact recovery requires distinguishing much smaller distances between candidate alignments, which in turn necessitates stronger correlation and thus a stronger condition.

For the special case $r = 0$, (Wu et al., 2022) shows that in the correlated Gaussian Wigner model, there is a phase transition from possible exact recovery to impossible recovery as the quantity $\frac{n \log(1/(1-\rho^2))}{\log n}$ changes from $4 + \epsilon$ to $4 - \epsilon$. For another special case $\rho = 0$, (Dai et al., 2019a) demonstrates that in the Gaussian database model exact recovery is possible when $d \log(1/(1-\rho^2)) \geq (4 + \epsilon) \log n$, and impossible when $d \log(1/(1-\rho^2)) \leq (4 - \epsilon) \log n$, under the same condition on the feature dimension d . In our new model $\mathcal{G}(n, d, \rho, r)$, we show that the optimal threshold is determined by the two components of the model: structure and features. Specifically, the term $n \log(1/(1-\rho^2))$ captures the contribution of structural information, while $d \log(1/(1-r^2))$ captures the contribution of feature information. Indeed, when $n \log(1/(1-\rho^2)) = C_1 \log n$ and $d \log(1/(1-r^2)) = C_2 \log n$ with $C_1, C_2 < 4$, and $C_1 + C_2 > 4$, there exists an estimator $\hat{\pi}$ that achieves exact recovery only when both edge and feature information are available. This demonstrates that our approach goes beyond the performance attainable by relying on either structural or feature information alone.

1.2 RELATED WORK

Attributed graph alignment In the information-theoretic perspective, Zhang et al. (2024) proposed the attributed Erdős-Rényi pair model, where the edges and the features follows Bernoulli distribution under a latent bijective mapping, and it derived the information-theoretic thresholds for recovering the latent mappings in both possibility and impossibility regimes. Yang & Chung (2024) proposed the correlated Gaussian-attributed Erdős-Rényi model and derived the optimal information-theoretic thresholds for exact recovery by analyzing the k -core estimator. Both work proposed random graph model with additional feature and found that the graph matching becomes feasible in a wider regime through the information of attributed nodes. There are also many algorithms on attributed in attributed graph alignment, including methods based on subgraph counting (Du et al., 2017; Liu et al., 2019; Wang et al., 2025), spectral methods (Zhang & Tong, 2016), optimal transport (Tang et al., 2023), and neighborhood statistics (Wang et al., 2024).

Other graph models Many information-theoretic properties of the correlated Gaussian Wigner model and correlated Erdős-Rényi model have been extensively investigated (Cullina & Kiyavash, 2016; 2017; Ganassali et al., 2021; Wu et al., 2022; 2023; Ding & Du, 2023b;a; Hall & Massoulié, 2023; Huang et al., 2024; Du, 2025; Huang & Yang, 2025), along with a rich line of algorithmic developments (Babai et al., 1980; Bollobás, 1982; Barak et al., 2019; Dai et al., 2019b; Ganassali & Massoulié, 2020; Ding et al., 2021; Mao et al., 2021; Piccioli et al., 2022; Mao et al., 2023a;c; Fan et al., 2023a;b; Ding & Li, 2023; 2024; Araya et al., 2024; Ganassali et al., 2024; Muratori & Semerjian, 2024; Du et al., 2025). However, the marginal distributions inherent in these models makes it different from graph models in practical applications. Therefore, it is crucial to explore more general graph models, such as graphon model (Wolfe & Olhede, 2013; Gao et al., 2015), inhomogeneous graph model (Rácz & Sridhar, 2023; Song et al., 2023; Ding et al., 2025), geometric random graph model (Wang et al., 2022; Bangachev & Bresler, 2024; Gong & Li, 2024; Sentenac et al., 2025), planted cycle model (Mao et al., 2023b; 2024), and multiple graph model (Ameen & Hajek, 2024; 2025).

2 POSSIBILITY RESULTS

We first introduce our estimator. Given two graphs $(G_1, G_2) \sim \mathcal{G}(n, d, \rho, r)$ under the featured correlated Gaussian Wigner model, our goal is design an estimator $\hat{\pi}(G_1, G_2)$ to recover the latent bijective mapping $\pi^* : V(G_1) \mapsto V(G_2)$. Let \mathcal{P} denote the joint distribution of (G_1, G_2) , $P(\cdot, \cdot)$

denote the distribution of two correlated standard normals with correlation ρ , and $f(\cdot, \cdot)$ denote the multivariate normal distribution $\mathcal{N}(0, \Sigma_d)$ with $\Sigma_d = \begin{bmatrix} I_d & rI_d \\ rI_d & I_d \end{bmatrix}$. Then the likelihood function is

$$\begin{aligned} \mathcal{P}_{G_1, G_2 | \pi^*} &= \prod_{e \in E(G_1)} P(\beta_e(G_1), \beta_{\pi^*(e)}(G_2)) \prod_{v \in V(G_1)} f(\mathbf{x}_v, \mathbf{y}_{\pi^*(v)}) \\ &\stackrel{(a)}{\propto} \exp \left(\frac{\rho}{1 - \rho^2} \sum_{e \in E(G_1)} \beta_e(G_1) \beta_{\pi^*(e)}(G_2) + \frac{r}{1 - r^2} \sum_{v \in V(G_1)} \mathbf{x}_v \mathbf{y}_{\pi^*(v)} \right), \end{aligned} \quad (1)$$

where (a) is because the quantities $\sum_{e \in E(G_1)} (\beta_e(G_1))^2$, $\sum_{e \in E(G_2)} (\beta_e(G_2))^2$, $\sum_{v \in V(G_1)} \mathbf{x}_v^\top \mathbf{x}_v$, and $\sum_{v \in V(G_1)} \mathbf{y}_{\pi^*(v)}^\top \mathbf{y}_{\pi^*(v)}$ are fixed given (G_1, G_2) . Consequently, our estimator takes the form

$$\hat{\pi} \in \arg \max_{\pi} \left\{ \frac{\rho}{1 - \rho^2} \sum_{e \in E(G_1)} \beta_e(G_1) \beta_{\pi(e)}(G_2) + \frac{r}{1 - r^2} \sum_{v \in V(G_1)} \mathbf{x}_v \mathbf{y}_{\pi(v)} \right\}. \quad (2)$$

Let $\varphi(x) = \frac{x}{1-x^2}$ and $S_\pi(G_1, G_2) = \varphi(\rho) \sum_{e \in E(G_1)} \beta_e(G_1) \beta_{\pi(e)}(G_2) + \varphi(r) \sum_{v \in V(G_1)} \mathbf{x}_v \mathbf{y}_{\pi(v)}$. Indeed, $S_\pi(G_1, G_2)$ represents the similarity score under π between G_1 and G_2 . Then the estimator is equivalent to $\hat{\pi} \in \arg \max_{\pi} S_\pi(G_1, G_2)$. For any two bijections $\pi, \pi' : V(G_1) \mapsto V(G_2)$, let $d(\pi, \pi') = n(1 - \text{overlap}(\pi, \pi'))$. To prove the successful recovery of $\hat{\pi}$, it suffices to show that

$$S_{\pi^*}(G_1, G_2) > \max_{\pi: d(\pi, \pi^*) \geq d_0} S_\pi(G_1, G_2) = \max_{k \geq d_0} \max_{\pi: d(\pi, \pi^*) = k} S_\pi(G_1, G_2)$$

with high probability, where the thresholds $d_0 = 1$ and $d_0 = (1 - \delta)m$ correspond to the exact and partial recoveries, respectively. Let \mathcal{T}_k denote the set of bijective mappings such that $d(\pi, \pi^*) = k$. Then the failure event satisfies

$$\{d(\hat{\pi}, \pi^*) = k\} \subseteq \{\exists \pi' \in \mathcal{T}_k : S_{\pi'}(G_1, G_2) \leq S_{\pi^*}(G_1, G_2)\}.$$

Accordingly we bound $\mathbb{P}[d(\hat{\pi}, \pi^*) = k]$ separately for large and small values of k . The next two propositions provide those bounds.

Proposition 1. *If $d = \omega(\log n)$ and $n \log \left(\frac{1}{1-\rho^2} \right) + 2d \log \left(\frac{1}{1-r^2} \right) \geq (4 + \epsilon) \log n$ with some constant $0 < \epsilon < 1$, then for any constant $0 < \delta < 1$ and $k \geq \delta n$, there exists $\hat{\pi}$ such that*

$$\mathbb{P}[d(\hat{\pi}, \pi^*) = k] \leq \exp \left(-nh \left(\frac{k}{n} \right) \right) \mathbf{1}_{\{k \leq n-1\}} + \exp(-2 \log n) \mathbf{1}_{\{k=n\}} + \exp \left(-\frac{\epsilon k \log n}{32} \right),$$

where $h(x) = -x \log x - (1-x) \log(1-x)$ is the binary entropy function.

In view of Proposition 1, an upper bound is established for any $d(\hat{\pi}, \pi^*) = k$ with $k \geq \delta n$. Summing over all $k \geq \delta n$ yields an error estimate for $\mathbb{P}[\text{overlap}(\hat{\pi}, \pi^*) \geq \delta]$ in the partial recovery regime. However, the proposition only controls the error probability when $k \geq \delta n$. To derive an error bound in the exact recovery regime, it remains necessary to handle the case $k < \delta n$. Specifically, we establish the following proposition.

Proposition 2. *If $n \log \left(\frac{1}{1-\rho^2} \right) + d \log \left(\frac{1}{1-r^2} \right) \geq (4 + \epsilon) \log n$ with some constant $0 < \epsilon < 1$, then for any $k \leq \frac{\epsilon}{16} n$, the estimator $\hat{\pi}$ in equation 2 satisfies*

$$\mathbb{P}[d(\hat{\pi}, \pi^*) = k] \leq \exp \left(-\frac{\epsilon}{8} k \log n \right).$$

The proofs of Propositions 1 and 2 are deferred to Appendices C.1 and C.2, respectively. By combining these two propositions, we obtain the possibility results stated in Theorems 1 and 2, through summing over $k \geq \delta n$ and $k \geq 1$, respectively. **The main task behind Propositions 1 and 2 is to control the MLE score difference $Z_\pi = S_\pi(G_1, G_2) - S_{\pi^*}(G_1, G_2)$ uniformly over all permutations under a mixed Gaussian channel (continuous edges and high-dimensional features). For permutations with macroscopic Hamming distance, we adapt the cycle decomposition and Gaussian moment-generating-function computation from Wu et al. (2022) to this structural-feature setting, obtaining sharp bounds with exponent $n \log(1/(1-\rho^2)) + 2d \log(1/(1-r^2))$. For permutations very close to π^* , we represent $S_{\pi^*} - S_\pi$ as a quadratic form in a jointly Gaussian vector (edges and features together), decorrelate the coordinates, and apply the Hanson-Wright inequality (Hanson & Wright, 1971) to get uniform bounds and the sharp constant in the exact recovery threshold.**

3 IMPOSSIBILITY RESULTS

In this section, we present information-theoretic impossibility results for the graph alignment problem. For the converse arguments, we adopt a Bayesian formulation by endowing the ground-truth permutation π^* with the uniform prior on \mathcal{S}_n ; under this prior, the MLE $\hat{\pi}$ minimizes the error probability among all estimators. To prove the impossibility results, it suffices to prove the failure of MLE, which corresponds to show the existence of a permutation π' that achieves a higher likelihood than the true permutation π^* . However, such strategy only proves impossibility results for exact recovery regime (See Proposition 4). We will show the impossibility results for the partial recovery regime by Fano’s method (see, e.g. (Cover & Thomas, 2006, Section 2.10)).

Let M_δ be a packing set of \mathcal{S}_n such that two distinct elements $\pi, \pi' \in M_\delta$ differs from a certain threshold. Specifically, we choose $\min_{\pi \neq \pi' \in M_\delta} d(\pi, \pi') > (1 - \delta)n$ in partial recovery regime and $M_1 = \mathcal{S}_n$. The cardinality of M_δ measures the complexity of the parameter space under the corresponding metric. Let \mathcal{P} denote the joint distribution of (G_1, G_2) , \mathcal{Q} be any distribution over (G_1, G_2) , and D_{KL} denote the Kullback–Leibler (KL) divergence. Then, the mutual information $I(\pi^*; G_1, G_2)$ can be upper bounded by

$$I(G_1, G_2; \pi^*) = \mathbb{E}_{\pi^*} [D_{\text{KL}}(\mathcal{P}_{G_1, G_2 | \pi^*} \| \mathcal{P}_{G_1, G_2})] \leq \max_{\pi \in \mathcal{S}_n} D_{\text{KL}}(\mathcal{P}_{G_1, G_2 | \pi} \| \mathcal{Q}_{G_1, G_2}),$$

where the inequality is because

$$D_{\text{KL}}(\mathcal{P}_{G_1, G_2 | \pi^*} \| \mathcal{P}_{G_1, G_2}) = D_{\text{KL}}(\mathcal{P}_{G_1, G_2 | \pi^*} \| \mathcal{Q}_{G_1, G_2}) - D_{\text{KL}}(\mathcal{P}_{G_1, G_2} \| \mathcal{Q}_{G_1, G_2})$$

and the KL divergence $D_{\text{KL}}(\mathcal{P}_{G_1, G_2} \| \mathcal{Q}_{G_1, G_2}) \geq 0$ for any distribution \mathcal{Q} . By Fano’s inequality, with π^* being the discrete uniform prior in the packing set M_δ , for any estimator $\hat{\pi}$, we have

$$\mathbb{P}[\text{overlap}(\hat{\pi}, \pi^*) < \delta] \geq 1 - \frac{I(\pi^*; G_1, G_2) + \log 2}{\log |M_\delta|}. \quad (3)$$

Specifically, we have the following Lemma on $|M_\delta|$ and $I(\pi^*; G_1, G_2)$.

Lemma 1. *For any $0 < \delta \leq 1$, we have*

$$|M_\delta| \geq \left(\frac{\delta n}{e}\right)^{\delta n}, \quad I(\pi^*; G_1, G_2) \leq \frac{1}{2} \binom{n}{2} \log \left(\frac{1}{1 - \rho^2}\right) + \frac{nd}{2} \log \left(\frac{1}{1 - r^2}\right). \quad (4)$$

In view of Lemma 1, $n \log(\frac{1}{1 - \rho^2})$ and $d \log(\frac{1}{1 - r^2})$ correspond to the mutual information contributed by the graph structure and the by the node features, respectively. Since the edges and features are independent, the total mutual information is given by the sum $n \log(\frac{1}{1 - \rho^2}) + d \log(\frac{1}{1 - r^2})$. The proof of Lemma 1 is deferred to Appendix D.1. Fano’s method lower bounds the Bayesian risk under the discrete uniform prior π^* on M_δ , which in turn also lower bounds the minimax risk. In particular, by combining Fano’s inequality in equation 3 with the relation in equation 4 in Lemma 1, we obtain the impossibility result for partial recovery with any constant $\delta \in (0, 1]$, as stated below.

Proposition 3 (Impossibility result, partial recovery). *For any $0 < \delta \leq 1$, if $n \log(\frac{1}{1 - \rho^2}) + 2d \log(\frac{1}{1 - r^2}) \leq c \log n$ for some constant c , then*

$$\mathbb{P}[\text{overlap}(\hat{\pi}, \pi^*) < \delta] \geq 1 - \frac{c}{4\delta}.$$

Proposition 3 provides an impossibility result for partial recovery, highlighting the relationship between the recovery probability and the threshold. This result also extends to the exact recovery regime when $\delta = 1$. The following proposition strengthens this conclusion under an assumption for the exact recovery regime, achieving both vanishing error and a sharp constant in the threshold.

Proposition 4 (Impossibility result, exact recovery). *If $n \log(\frac{1}{1 - \rho^2}) + d \log(\frac{1}{1 - r^2}) + 4 \log d \leq (4 - \epsilon) \log n$ for some constant $\epsilon > 0$ under the assumption $r^2 \geq \frac{40}{d}$, then for any estimator $\hat{\pi}$,*

$$\mathbb{P}[\hat{\pi} \neq \pi^*] = 1 - o(1).$$

By Proposition 4, we derive sharp information-theoretic thresholds for exact recovery with a gap of $4 \log d$. The proofs of Propositions 3 and 4 are deferred to Appendices C.3 and C.4, respectively.

4 QPALIGN: QUADRATIC PROGRAMMING RELAXATION FOR ATTRIBUTED GRAPH ALIGNMENT

In Sections 2 and 3, we have shown that the MLE in equation 2 achieves the optimal information-theoretic thresholds. However, this estimator requires an exhaustive search over all possible mappings in \mathcal{S}_n , which has a runtime of order $n!$. To address this computational bottleneck, we propose QPALign, an approximation algorithm for attributed graph alignment.

Let $[n] \triangleq \{1, 2, \dots, n\}$. Without loss of generality, we assume $V(G_1) = V(G_2) = [n]$, $\pi : [n] \mapsto [n]$ and $E(G_1) = E(G_2) = \{(i, j) : 1 \leq i < j \leq n\}$. Let Π be the permutation matrix of π with $\Pi_{ij} = \mathbf{1}_{\{\pi(i)=j\}}$ for any $1 \leq i, j \leq n$, and define $\lambda \triangleq \frac{\varphi(\rho)}{\varphi(\rho) + \varphi(\tau)}$. Then the MLE $\hat{\pi}$ in equation 2 is equivalent to minimizing

$$\lambda \sum_{1 \leq i < j \leq n} (\beta_{ij}(G_1) - \beta_{\pi(i)\pi(j)}(G_2))^2 + (1 - \lambda) \sum_{1 \leq i \leq n} \|\mathbf{x}_i - \mathbf{y}_{\pi(i)}\|^2. \quad (5)$$

Denote A_1, A_2 as the adjacent matrices of G_1, G_2 . Let $B_1^i = \text{diag}\{\mathbf{x}_{1i}, \mathbf{x}_{2i}, \dots, \mathbf{x}_{ni}\}$ and $B_2^i = \text{diag}\{\mathbf{y}_{1i}, \mathbf{y}_{2i}, \dots, \mathbf{y}_{ni}\}$ for any $i \in [d]$, where \mathbf{x}_{ki} corresponds to the i -component of vector \mathbf{x}_k . Then equation 5 is equivalent to

$$\begin{aligned} & \lambda \|A_1 - \Pi A_2 \Pi^\top\|_F^2 + (1 - \lambda) \sum_{i=1}^d \|B_1^i - \Pi B_2^i \Pi^\top\|_F^2 \\ &= \lambda \|A_1 \Pi - \Pi A_2\|_F^2 + (1 - \lambda) \sum_{i=1}^d \|B_1^i \Pi - \Pi B_2^i\|_F^2 \triangleq f(\Pi), \end{aligned} \quad (6)$$

where $\Pi \in \mathbb{P}^n \triangleq \{\mathbf{P} \in \{0, 1\}^{n \times n}, \mathbf{P}\mathbf{1} = \mathbf{1}, \mathbf{P}^\top \mathbf{1} = \mathbf{1}\}$. Indeed, this is an instance of the *quadratic assignment problem* (QAP) (Pardalos et al., 1994; Burkard et al., 1998), which is NP-hard to solve or to approximate (Makarychev et al., 2010). To obtain a computationally efficient algorithm for estimating $\hat{\pi}$, we employ a relaxation approach. Relaxing the set of permutations to Birkhoff polytope (the set of doubly stochastic matrices)

$$\mathbb{W}^n \triangleq \{\mathbf{W} \in [0, 1]^{n \times n} : \mathbf{W}\mathbf{1} = \mathbf{1}, \mathbf{W}^\top \mathbf{1} = \mathbf{1}, 0 \leq \mathbf{W}_{ij} \leq 1 \text{ for all } i, j\},$$

we derive the quadratic programming (QP) relaxation

$$\min_{\Pi \in \mathbb{W}^n} \left\{ \lambda \|A_1 \Pi - \Pi A_2\|_F^2 + (1 - \lambda) \sum_{i=1}^d \|B_1^i \Pi - \Pi B_2^i\|_F^2 \right\}. \quad (7)$$

We solve the above quadratic programming by projected gradient descent. Specifically, we project the matrix to \mathbb{W}_n by Euclidean projection: $\Pi^{k+1} = \text{Proj}_{\mathbb{W}_n}(\Pi^k - \eta \nabla f(\Pi^k))$, where η is the step size. We have the following Theorem on the convergence guarantee for the gradient descent method.

Theorem 3. *For any two graphs G_1, G_2 , there exists a universal constant $L = L(G_1, G_2)$ such that, for function f defined in equation 6 and any $\eta \leq L^{-1}$, we have*

$$|f(\Pi^K) - f(\Pi')| \leq \frac{1}{2\eta K} \|\Pi^0 - \Pi'\|_F^2 \leq \frac{n}{\eta K}$$

for any integer $K \geq 1$, where $\Pi' \in \arg \min_{\Pi \in \mathbb{W}^n} f(\Pi)$ and Π^0 is the initial state.

Indeed, relaxing to Birkhoff polytope is widely adopted in graph matching (Vogelstein et al., 2015; Bommakanti et al., 2024), and has been proved tight in random graph models (Fan et al., 2023a;b). In practice, we often regard λ as a tuning parameter and adapt model selection technique for picking λ . See Remark 1 for further details. In view of Theorem 3, we obtain a standard $O(1/K)$ convergence guarantee for the projected gradient descent scheme with exact Euclidean projections onto \mathbb{W}_n . However, in our implementation, we replace these exact projections by a few iterations of Sinkhorn scaling (Sinkhorn, 1964) as a fast approximate projection onto \mathbb{W}_n . In practice, since Sinkhorn requires nonnegative entries, we apply it to the truncated matrix $(\Pi^{(t+1)})_+$, obtained by setting all negative entries of $\Pi^{(t+1)}$ to zero.

Define $D \in \mathbb{R}^{n \times n}$ as $D_{kj} = \|\mathbf{x}_k - \mathbf{y}_j\|_2^2$. We note that $\sum_{i=1}^d \|B_1^i \Pi - \Pi B_2^i\|_F^2 = \sum_{k,j} D_{kj} \Pi_{kj}^2$. Note that $\sum_{k,j} \Pi_{kj}(1 - \Pi_{kj}) = 0$ for permutation matrix Π . We turn this constraint into a regularizer with parameter μ and derive the following program:

$$\min_{\Pi \in \mathbb{W}^n} \left\{ \lambda \|A_1 \Pi - \Pi A_2\|_F^2 + (1 - \lambda) \sum_{k,j} D_{kj} \Pi_{kj}^2 + \mu \sum_{k,j} \Pi_{kj}(1 - \Pi_{kj}) \right\}. \quad (8)$$

We solve the problem in equation 8 by QPAlign in Algorithm 1. In the following, we outline a general recipe for QPAlign.

- *Gradient descent.* We update $\Pi^{(t+1)} = \Pi^{(t)} - \eta G^{(t)}$ with step size $\eta > 0$, where the gradient is given by

$$G^{(t)} = 2\lambda(A_1^\top E - EA_2^\top) + 2(1 - \lambda) \left(D \circ \Pi^{(t)} \right) + \mu \left(J_{n \times n} - 2\Pi^{(t)} \right),$$

where $E = A_1 \Pi^{(t)} - \Pi^{(t)} A_2$ and $(D \circ \Pi^{(t)})_{ij} = D_{ij} \Pi_{ij}^{(t)}$, $J_{ij} = 1$ for any i, j .

- *Sinkhorn normalization.* After each gradient step, update $\Pi^{(t+1)}$ on the set of doubly stochastic matrices \mathbb{W}^n using K iterations of the Sinkhorn normalization procedure (Sinkhorn, 1964).
- *Rounding via Hungarian algorithm.* Once convergence is reached, the final doubly stochastic matrix is converted into a permutation matrix by solving the matching problem $\arg \max_{\pi \in \mathcal{S}_n} \sum_i \Pi_{i,\pi(i)}^{(t)}$ using the Hungarian algorithm (Kuhn, 1955; Munkres, 1957).

Time complexity The construction of the feature-distance matrix D requires $O(dn^2)$ time. Each gradient step has a complexity of $O(n^3)$, and the Sinkhorn algorithm with K iterations takes $O(Kn^3)$. Consequently, performing T iterations of gradient descent and Sinkhorn projection costs $O(TKn^3)$. The final rounding via the Hungarian algorithm requires $O(n^3)$ (Munkres, 1957). Overall, the time complexity of QPAlign is $O((d + TKn)n^2)$.

Algorithm 1 QPAlign: Quadratic Programming relaxation for attributed graph Alignment

- 1: **Input:** Adjacency matrices $A_1, A_2 \in \mathbb{R}^{n \times n}$; node features $\mathbf{x}_i, \mathbf{y}_i, 1 \leq i \leq n$; weights $\lambda, \mu > 0$; step size $\eta > 0$; Sinkhorn iters K ; max iters T ; tolerance tol.
 - 2: **Output:** Estimated permutation $\hat{\pi}$.
 - 3: Construct feature-distance matrix $D \in \mathbb{R}^{n \times n}$ with $D_{ij} = \|\mathbf{x}_i - \mathbf{y}_j\|_2^2$.
 - 4: Initialize $\Pi^{(0)}$.
 - 5: **for** $t = 0, \dots, T - 1$ **do**
 - 6: $E \leftarrow A_1 \Pi^{(t)} - \Pi^{(t)} A_2$.
 - 7: $f^{(t)} \leftarrow \lambda \|E\|_F^2 + (1 - \lambda) \sum_{i,j} D_{ij} (\Pi_{ij}^{(t)})^2 + \mu \sum_{i,j} \Pi_{ij}^{(t)} (1 - \Pi_{ij}^{(t)})$.
 - 8: $G^{(t)} \leftarrow 2\lambda(A_1^\top E - EA_2^\top) + 2(1 - \lambda) (D \circ \Pi^{(t)}) + \mu (J_{n \times n} - 2\Pi^{(t)})$.
 - 9: Gradient step: $\Pi^{(t+1)} \leftarrow \Pi^{(t)} - \eta G^{(t)}$.
 - 10: **Truncate negative entries:** $\Pi^{(t+1)} \leftarrow (\Pi^{(t+1)})_+, (\cdot)_+:$ elementwise $\max\{\cdot, 0\}$.
 - 11: Update $\Pi^{(t+1)}$ on the Birkhoff polytope via Sinkhorn: $\Pi^{(t+1)} \leftarrow \text{Sinkhorn}((\Pi^{(t+1)})_+, K)$.
 - 12: **if** $t > 0$ and $|f^{(t)} - f^{(t-1)}| < \text{tol}$ **then**
 - 13: **break**
 - 14: **end if**
 - 15: **end for**
 - 16: Round to a permutation via Hungarian algorithm: $\hat{\pi} \leftarrow \arg \max_{\pi \in \mathcal{S}_n} \sum_i \Pi_{i,\pi(i)}^{(t)}$.
 - 17: **return** $\hat{\pi}$.
-

Remark 1 (Tuning parameter). *In practice, when solving the quadratic program in equation 8, the parameter λ is typically difficult to estimate from the observations G_1 and G_2 . Hence, both λ and μ are usually treated as tuning parameters. One strategy for selecting them is cross-validation. Although we only have a single graph pair (G_1, G_2) , one can apply the algorithm to several randomly sampled subgraphs and choose the values of λ and μ that minimize the average validation loss.*

Remark 2 (Regularization term). We add a regularization term $\sum_{k,j} \Pi_{kj}(1 - \Pi_{kj})$ in program 8. This term encourages the entries of Π to approach 0 or 1. While some previous works employ a penalty of the form $\|\Pi\|_F^2$ to obtain an explicit solution (see, e.g. Fan et al. (2020)), our relaxation directly pushes the solution toward the boundary of the Birkhoff polytope. As a result, the intermediate matrix $\Pi^{(t)}$ becomes more concentrated near the vertices of the Birkhoff polytope, which allows the final rounding via the Hungarian algorithm to be more precise. Therefore, the inclusion of this regularization term helps to improve the overall accuracy of the estimated permutation $\hat{\pi}$.

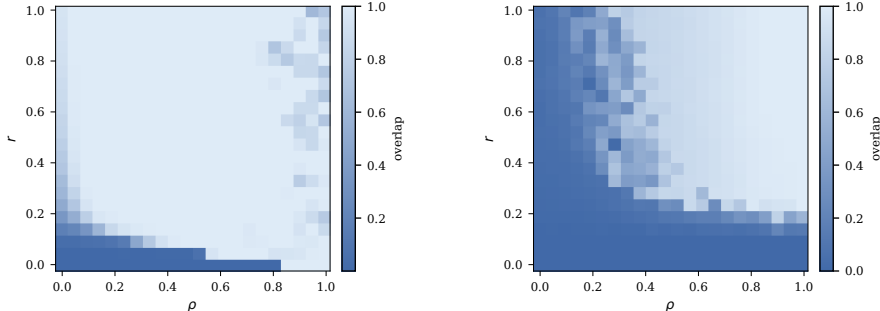
5 NUMERICAL RESULTS

5.1 SIMULATION STUDIES

In this subsection, we provide numerical results for QPAlign in Algorithm 1 on synthetic data. One related model is the correlated Gaussian-attributed Erdős-Rényi model (Yang & Chung, 2024), where the correlated pairs of edges follow a multivariate Bernoulli distribution with connection probability p and correlation ρ . Fixing $n = 3000$ and $d = 512$ (with $p = 0.5$ in the Erdős-Rényi case), we run the algorithm and report the value of $\text{overlap}(\hat{\pi}, \pi^*)$ for varying correlations $\rho \in [0, 1]$ and $r \in [0, 1]$. We evaluate our method with step size $\eta = 10^{-4}$, $T = 400$, $K = 80$, $\lambda = 0.1$ and $\mu = 0.1$ for the experiments reported here.

Our results are summarized in Figure 1. Figure 1a displays the heatmap of the overlap under the featured correlated Gaussian Wigner model. We observe that the overlap increases smoothly with both ρ and r , starting from nearly zero when both correlations vanish and approaching one when both correlations are close to unity. This indicates that the estimator $\hat{\pi}$ gradually aligns with the ground truth π^* as the signal in either edges or features becomes stronger. For the low-dimensional setting with $n = 100$ and $d = 16$, we present additional results in Figure 4 in Appendix A.1, which exhibit the same qualitative trend, confirming the effectiveness of our method in both regimes. Importantly, these numerical results are consistent with the information-theoretic exact recovery thresholds given in Theorem 2. We also note that in certain intermediate regimes, there exists a statistic-computation gap: while exact recovery is theoretically possible, computationally achieving it may require stronger correlations. See Figure 5 in Appendix A.1 for a more detailed comparison between the information-theoretic thresholds and the empirical phase-transition boundaries of QPAlign.

Figure 1b shows the corresponding result under the featured correlated Erdős-Rényi model with $p = 0.5$. A qualitatively similar pattern is observed: the algorithm achieves high overlap once either ρ or r is sufficiently large. Together, these experiments confirm that our algorithm behaves stably across different correlation regimes and successfully interpolates between weak and strong signal cases, with $\text{overlap}(\hat{\pi}, \pi^*)$ ranging from 0 to 1 as (ρ, r) varies from $(0, 0)$ to $(1, 1)$. The results show that our approach is effective for both weighted and unweighted graphs, which broadens the applicability relative to prior methods. See more comparisons with the benchmarks in Appendix A.1.



(a) Featured correlated Gaussian Wigner model with $n = 3000$ and $d = 512$.

(b) Featured correlated Erdős-Rényi model with $n = 3000$, $d = 512$, and $p = 0.5$.

Figure 1: Overlap between the estimator $\hat{\pi}$ in Algorithm 1 and the ground truth π^* in two models with $n = 3000$ and $d = 512$, evaluated across varying correlations $\rho \in [0, 1]$ and $r \in [0, 1]$.

5.2 REAL DATA ANALYSIS

ACM-DBLP dataset The ACM-DBLP dataset (Tang et al., 2008) is a widely used benchmark for attributed graph alignment, containing 2,224 ground-truth matched pairs. In our construction, each node represents a paper from either the ACM or DBLP source, and edges are weighted by co-authorship relations. The ground-truth alignment is given by the set of papers appearing in both sources. We implemented the experiments with hyperparameters $\mu = 0.01$, $T = 1000$, $K = 200$, step size $\eta = 10^{-5}$, and $\lambda \in \{0, 0.2, 0.4, 0.6, 0.8, 1\}$.

Douban (Online–Offline) dataset The Douban Online–Offline dataset (Tang et al., 2008) is another widely used benchmark for attributed graph alignment, consisting of two graphs that share 1,118 ground-truth matched pairs. Each node represents a user, with edges in the online graph encoding platform interactions (e.g., replying to a post) and edges in the offline graph capturing co-attendance at social events. Node features are given by user locations. The online graph strictly contains all users from the offline graph, and the ground-truth alignment is defined by the users present in both. We implemented the experiments with hyperparameters $\mu = 0$, $T = 1000$, $K = 200$, step size $\eta = 5 \times 10^{-3}$, and $\lambda \in \{0, 0.2, 0.4, 0.6, 0.8, 1\}$.

Indeed, the ACM-DBLP dataset corresponds to a featured Gaussian-Wigner graph, while the Douban dataset is treated as a featured Erdős-Rényi graph, each representing different structural settings for graph alignment. We compare our method with three types of baselines: 1) based solely on edge structure (Grampa (Fan et al., 2023a), IsoRank (Singh et al., 2008), Umeyama (Umeyama, 1988), GW (Peyré et al., 2016)); 2) based solely on node features (MAP (Dai et al., 2019a), kNN); and 3) exploiting both edge structure and node features (FGW (Titouan et al., 2019), REGAL (Heimann et al., 2018), PARROT (Zeng et al., 2023)). To ensure a fair comparison, we follow the official implementations and parameter choices recommended in the original papers. Since the baselines are designed for different settings (edge-only, feature-only, or joint), [the results should be viewed within their respective information settings rather than as direct head-to-head comparisons.](#)

The results are reported in Figure 2 and Table 1. We report the experimental results averaged over 5 random seeds. The faint curves represent the results of individual runs, while the bold curves show their average. To fairly compare with baselines using the corresponding information source in Table 1, we conducted two ablated versions: $\lambda = 0$, which corresponds to using only feature information, and $\lambda = 1$, which corresponds to using only edge information. The results in Figure 2 and Table 1 both demonstrate that combining the two sources of information yields performance that surpasses relying on either source alone. See more details in Appendix A.2.

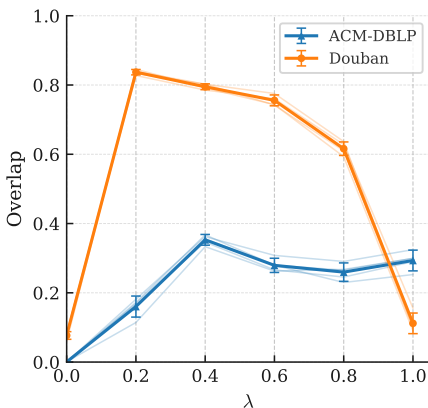


Figure 2: Overlap vs. λ on ACM-DBLP and Douban datasets.

	ACM-DBLP	Douban
QAlign (max)	0.3445	0.8370
FGW	0.0018	0.2773
REGAL	0.0301	0.1118
PARROT	0.0441	0.8462
QAlign ($\lambda = 0$)	0.0004	0.0767
MAP	0.0004	0.0411
kNN	0.0004	0.0725
QAlign ($\lambda = 1$)	0.2896	0.1118
Grampa	0.0746	0.0027
IsoRank	0.0018	0.0000
Umeyama	0.0346	0.0089
GW	0.0202	0.0000

Table 1: Experimental results in alignment across ACM-DBLP and Douban datasets.

Spatial transcriptomic dataset Spatial transcriptomic (ST) data (Ståhl et al., 2016) consist of gene expression profiles measured at spatially localized spots on a tissue slice, where each feature corresponds to a gene and the spatial coordinates represent the physical locations of the spots. We

use an ST slice containing 255 spots with 7,998 gene features as the base dataset. To enable quantitative evaluation with ground-truth correspondences, we generate simulated slices by rotating the spot coordinates and resampling expression counts after adding a pseudocount δ to each gene in each spot. We consider five noise levels ($\delta \in 0, 1, 2, 3, 4, 5$) to model increasing experimental variability. The detailed procedure of data construction is provided in Appendix A.3.

In the experiment, we further examined the sensitivity of our method with respect to λ . Recall that $\lambda = 0$ corresponds to using only the feature information, while $\lambda = 1$ corresponds to relying solely on the structural information. Across the entire range of λ , our method consistently achieved strong alignment performance, indicating remarkable robustness to the choice of λ . In comparison with widely adopted baselines for spatial transcriptomics data alignment, including BBKNN (Polański et al., 2020) and Harmony (Korsunsky et al., 2019), our approach yields consistently superior results. We implemented the experiments with parameters $T = 400$, $K = 80$, $\mu = 0.1$, $\eta = 10^{-5}$.

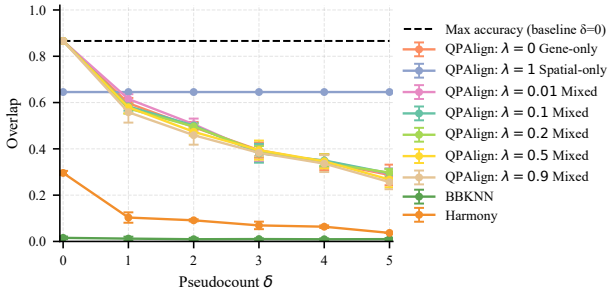


Figure 3: Alignment accuracy across different values of λ in ST data

6 CONCLUSIONS

In this paper, we study the graph alignment problem under a featured Gaussian Wigner model, where two graphs follow a Gaussian Wigner model and each node is equipped with correlated Gaussian feature vectors. We derive rate-optimal information-theoretic thresholds for both partial and exact recovery in this setting. In addition, we propose QPAlign, a fast algorithm based on a quadratic programming relaxation over the Birkhoff polytope. Our main contributions are as follows.

- *Information-theoretic thresholds.* We establish the optimal rates for both partial recovery and exact recovery regimes. Furthermore, in the regime where $d = n^{o(1)}$ and $d = \omega(\log n)$, our thresholds for exact recovery are sharp up to a constant factor. The results are mainly depends on the analysis of the MLE, where a careful option for the weight on feature and edge is selected to obtain the optimal results.
- *Algorithm and validation on real datasets.* We introduce QPAlign, a quadratic-programming-based relaxation with a penalty term in equation 1 that encourages permutation-like solutions while remaining computationally efficient. We demonstrate the effectiveness of QPAlign on both synthetic and real attributed networks, where it achieves high-quality alignments and compares favorably with existing baselines.

Beyond the main contributions, there are also several important directions merit further explorations.

- *Dependencies between edges and features.* In our featured Gaussian Wigner model, the structural and feature channels are modeled in a relatively simple way. One generalization is to allow richer joint distributions in which edges and node features are generated from a common latent source, so that the edge variables may explicitly depend on the features.
- *Generalization to other graph models.* A natural direction is to extend the framework to more realistic random graph models with attributes, such as inhomogeneous Erdős-Rényi graphs (Ding et al., 2025), stochastic block models with community structure (Onaran et al., 2016; Yang & Chung, 2025), or more general graphon models (Gao et al., 2015). It is of interest to understand whether similar results continue to hold in these broader settings.

540 ETHICS STATEMENT

541
542 Our research is entirely theoretical and experimental on synthetic data and publicly available
543 datasets. We are not aware of any ethical concerns related to discrimination, privacy, security, or
544 misuse. All results are presented with academic integrity, and there are no conflicts of interest or
545 sponsorship issues associated with this work.

546 REPRODUCIBILITY STATEMENT

547
548 We have made every effort to ensure the reproducibility of our results. Theoretical claims are sup-
549 ported by complete proofs provided in the appendix. Experimental details, including data genera-
550 tion procedures, model parameters, and evaluation metrics, are fully described in the main text and
551 supplementary materials. To further facilitate verification, we submit a complete package of our
552 implementation and experiment scripts as supplementary material, which allows others to reproduce
553 all results reported in this paper.

554 REFERENCES

- 555
556 Taha Ameen and Bruce Hajek. Exact random graph matching with multiple graphs. *arXiv preprint*
557 *arXiv:2405.12293*, 2024.
- 559 Taha Ameen and Bruce Hajek. Detecting correlation between multiple unlabeled Gaussian net-
560 works. *arXiv preprint arXiv:2504.16279*, 2025.
- 562 Ernesto Araya, Guillaume Braun, and Hemant Tyagi. Seeded graph matching for the correlated
563 Gaussian Wigner model via the projected power method. *Journal of Machine Learning Research*,
564 25(5):1–43, 2024.
- 565 László Babai, Paul Erdős, and Stanley M Selkow. Random graph isomorphism. *SIAM Journal on*
566 *computing*, 9(3):628–635, 1980.
- 568 Kiril Bangachev and Guy Bresler. Detection of L_∞ Geometry in Random Geometric Graphs: Sub-
569 optimality of Triangles and Cluster Expansion. In *Proceedings of Thirty Seventh Conference on*
570 *Learning Theory*, pp. 427–497. PMLR, 2024.
- 571 Boaz Barak, Chi-Ning Chou, Zhixian Lei, Tselil Schramm, and Yueqi Sheng. (Nearly) efficient
572 algorithms for the graph matching problem on correlated random graphs. *Advances in Neural*
573 *Information Processing Systems*, 32, 2019.
- 575 Jonathan Barzilai and Jonathan M Borwein. Two-point step size gradient methods. *IMA journal of*
576 *numerical analysis*, 8(1):141–148, 1988.
- 577 Alexander C Berg, Tamara L Berg, and Jitendra Malik. Shape matching and object recognition using
578 low distortion correspondences. In *2005 IEEE computer society conference on computer vision*
579 *and pattern recognition (CVPR’05)*, volume 1, pp. 26–33. IEEE, 2005.
- 581 Z. W. Birnbaum. An inequality for Mill’s ratio. *The Annals of Mathematical Statistics*, 13(2):245 –
582 246, 1942.
- 583 Béla Bollobás. Distinguishing vertices of random graphs. In *North-Holland Mathematics Studies*,
584 volume 62, pp. 33–49. Elsevier, 1982.
- 586 Aditya Bommakanti, Harshith Vonteri, Konstantinos Skitsas, Sayan Ranu, Davide Mottin, and Pana-
587 giotis Karras. FUGAL: Feature-fortified Unrestricted Graph Alignment. *Advances in Neural*
588 *Information Processing Systems*, 37:19523–19546, 2024.
- 589 Rainer E Burkard, Eranda Cela, Panos M Pardalos, and Leonidas S Pitsoulis. The quadratic as-
590 signment problem. In *Handbook of Combinatorial Optimization: Volume 1–3*, pp. 1713–1809.
591 Springer, 1998.
- 592
593 Shuwen Chai and Miklós Z Rácz. Efficient graph matching for correlated stochastic block models.
Advances in Neural Information Processing Systems, 37:116388–116461, 2024.

- 594 Thomas M. Cover and Joy A Thomas. *Elements of Information Theory*. Wiley-Interscience, 2006.
- 595
- 596 Daniel Cullina and Negar Kiyavash. Improved achievability and converse bounds for Erdős-Rényi
597 graph matching. *ACM SIGMETRICS performance evaluation review*, 44(1):63–72, 2016.
- 598 Daniel Cullina and Negar Kiyavash. Exact alignment recovery for correlated Erdős-Rényi graphs.
599 *arXiv preprint arXiv:1711.06783*, 2017.
- 600
- 601 Osman E Dai, Daniel Cullina, and Negar Kiyavash. Database alignment with Gaussian features.
602 In *The 22nd International Conference on Artificial Intelligence and Statistics*, pp. 3225–3233.
603 PMLR, 2019a.
- 604 Osman Emre Dai, Daniel Cullina, Negar Kiyavash, and Matthias Grossglauser. Analysis of a canon-
605 ical labeling algorithm for the alignment of correlated Erdős-Rényi graphs. *Proceedings of the*
606 *ACM on Measurement and Analysis of Computing Systems*, 3(2):1–25, 2019b.
- 607
- 608 Jian Ding and Hang Du. Detection threshold for correlated Erdős-Rényi graphs via densest sub-
609 graph. *IEEE Transactions on Information Theory*, 69(8):5289–5298, 2023a.
- 610 Jian Ding and Hang Du. Matching recovery threshold for correlated random graphs. *The Annals of*
611 *Statistics*, 51(4):1718–1743, 2023b.
- 612
- 613 Jian Ding and Zhangsong Li. A polynomial-time iterative algorithm for random graph matching
614 with non-vanishing correlation. *arXiv preprint arXiv:2306.00266*, 2023.
- 615 Jian Ding and Zhangsong Li. A polynomial time iterative algorithm for matching Gaussian matrices
616 with non-vanishing correlation. *Foundations of Computational Mathematics*, pp. 1–58, 2024.
- 617
- 618 Jian Ding, Zongming Ma, Yihong Wu, and Jiaming Xu. Efficient random graph matching via degree
619 profiles. *Probability Theory and Related Fields*, 179:29–115, 2021.
- 620 Jian Ding, Yumou Fei, and Yuanzheng Wang. Efficiently matching random inhomogeneous graphs
621 via degree profiles. *The Annals of Statistics*, 53(4):1808–1832, 2025.
- 622
- 623 Boxin Du, Si Zhang, Nan Cao, and Hanghang Tong. First: Fast interactive attributed subgraph
624 matching. In *Proceedings of the 23rd ACM SIGKDD international conference on knowledge*
625 *discovery and data mining*, pp. 1447–1456, 2017.
- 626 Hang Du. Optimal recovery of correlated Erdős-Rényi graphs. *arXiv preprint arXiv:2502.12077*,
627 2025.
- 628
- 629 Hang Du, Shuyang Gong, and Rundong Huang. The algorithmic phase transition of random graph
630 alignment problem. *Probability Theory and Related Fields*, pp. 1–56, 2025.
- 631 Zhou Fan, Cheng Mao, Yihong Wu, and Jiaming Xu. Spectral graph matching and regularized
632 quadratic relaxations: Algorithm and theory. In *International conference on machine learning*,
633 pp. 2985–2995. PMLR, 2020.
- 634 Zhou Fan, Cheng Mao, Yihong Wu, and Jiaming Xu. Spectral graph matching and regularized
635 quadratic relaxations I: The Gaussian model. *Foundations of Computational Mathematics*, 23(5):
636 1511–1565, 2023a.
- 637
- 638 Zhou Fan, Cheng Mao, Yihong Wu, and Jiaming Xu. Spectral graph matching and regularized
639 quadratic relaxations II: Erdős-Rényi graphs and universality. *Foundations of Computational*
640 *Mathematics*, 23(5):1567–1617, 2023b.
- 641 Luca Ganassali and Laurent Massoulié. From tree matching to sparse graph alignment. In *Confer-*
642 *ence on Learning Theory*, pp. 1633–1665. PMLR, 2020.
- 643
- 644 Luca Ganassali, Laurent Massoulié, and Marc Lelarge. Impossibility of partial recovery in the graph
645 alignment problem. In *Conference on Learning Theory*, pp. 2080–2102. PMLR, 2021.
- 646
- 647 Luca Ganassali, Laurent Massoulié, and Guilhem Semerjian. Statistical limits of correlation detec-
tion in trees. *The Annals of Applied Probability*, 34(4):3701–3734, 2024.

- 648 Chao Gao, Yu Lu, and Harrison H Zhou. Rate-optimal graphon estimation. *The Annals of Statistics*,
649 43(6):2624–2652, 2015.
- 650
- 651 Malay Ghosh. Exponential tail bounds for chisquared random variables. *Journal of Statistical*
652 *Theory and Practice*, 15(2):35, 2021.
- 653 Shuyang Gong and Zhangsong Li. The Umeyama algorithm for matching correlated Gaussian geo-
654 metric models in the low-dimensional regime. *arXiv preprint arXiv:2402.15095*, 2024.
- 655
- 656 Aria Haghighi, Andrew Y Ng, and Christopher D Manning. Robust textual inference via graph
657 matching. In *Proceedings of Human Language Technology Conference and Conference on Em-*
658 *pirical Methods in Natural Language Processing*, pp. 387–394, 2005.
- 659 Georgina Hall and Laurent Massoulié. Partial recovery in the graph alignment problem. *Operations*
660 *Research*, 71(1):259–272, 2023.
- 661
- 662 David Lee Hanson and Farroll Tim Wright. A bound on tail probabilities for quadratic forms in
663 independent random variables. *The Annals of Mathematical Statistics*, 42(3):1079–1083, 1971.
- 664 Mark Heimann, Haoming Shen, Tara Safavi, and Danai Koutra. REGAL: representation learning-
665 based graph alignment. In *Proceedings of the 27th ACM International Conference on Information*
666 *and Knowledge Management*, pp. 117–126. ACM, 2018.
- 667
- 668 Roger A Horn and Charles R Johnson. *Matrix analysis*. Cambridge university press, 2012.
- 669 Dong Huang and Pengkun Yang. Sample complexity of correlation detection in the Gaussian Wigner
670 model. *arXiv preprint arXiv:2505.14138*, 2025.
- 671
- 672 Dong Huang, Xianwen Song, and Pengkun Yang. Information-theoretic thresholds for the align-
673 ments of partially correlated graphs. In *Conference on Learning Theory*, pp. 2494–2518. PMLR,
674 2024.
- 675 Ilya Korsunsky, Nghia Millard, Jean Fan, Kamil Slowikowski, Fan Zhang, Kevin Wei, Yuriy
676 Baglaenko, Michael Brenner, Po-ru Loh, and Soumya Raychaudhuri. Fast, sensitive and accurate
677 integration of single-cell data with Harmony. *Nature methods*, 16(12):1289–1296, 2019.
- 678
- 679 Harold W Kuhn. The Hungarian method for the assignment problem. *Naval research logistics*
680 *quarterly*, 2(1-2):83–97, 1955.
- 681 Dmitriy Kunisky and Jonathan Niles-Weed. Strong recovery of geometric planted matchings. In
682 *Proceedings of the 2022 Annual ACM-SIAM Symposium on Discrete Algorithms (SODA)*, pp.
683 834–876. SIAM, 2022.
- 684
- 685 Jure Leskovec, Daniel Huttenlocher, and Jon Kleinberg. Predicting positive and negative links in
686 online social networks. In *Proceedings of the 19th international conference on World wide web*,
687 pp. 641–650, 2010.
- 688 Lihui Liu, Boxin Du, Hanghang Tong, et al. G-finder: Approximate attributed subgraph matching.
689 In *2019 IEEE international conference on big data (big data)*, pp. 513–522. IEEE, 2019.
- 690
- 691 Zhuang Liu, Wayne Lin, Ya Shi, and Jun Zhao. A robustly optimized BERT pre-training approach
692 with post-training. In *China national conference on Chinese computational linguistics*, pp. 471–
693 484. Springer, 2021.
- 694 Vince Lyzinski. Information recovery in shuffled graphs via graph matching. *IEEE Transactions on*
695 *Information Theory*, 64(5):3254–3273, 2018.
- 696
- 697 Konstantin Makarychev, Rajsekar Manokaran, and Maxim Sviridenko. Maximum quadratic assign-
698 ment problem: Reduction from maximum label cover and lp-based approximation algorithm. In
699 *International Colloquium on Automata, Languages, and Programming*, pp. 594–604. Springer,
700 2010.
- 701 Cheng Mao, Mark Rudelson, and Konstantin Tikhomirov. Random graph matching with improved
noise robustness. In *Conference on Learning Theory*, pp. 3296–3329. PMLR, 2021.

- 702 Cheng Mao, Mark Rudelson, and Konstantin Tikhomirov. Exact matching of random graphs with
703 constant correlation. *Probability Theory and Related Fields*, 186(1-2):327–389, 2023a.
704
- 705 Cheng Mao, Alexander S Wein, and Shenduo Zhang. Detection-recovery gap for planted dense
706 cycles. In *The Thirty Sixth Annual Conference on Learning Theory*, pp. 2440–2481. PMLR,
707 2023b.
- 708 Cheng Mao, Yihong Wu, Jiaming Xu, and Sophie H Yu. Random graph matching at Otter’s threshold
709 via counting chandeliers. In *Proceedings of the 55th Annual ACM Symposium on Theory of
710 Computing*, pp. 1345–1356, 2023c.
711
- 712 Cheng Mao, Alexander S. Wein, and Shenduo Zhang. Information-theoretic thresholds for planted
713 dense cycles. *arXiv preprint arXiv:2402.00305*, 2024.
- 714 Diana Mateus, Radu Horaud, David Knossow, Fabio Cuzzolin, and Edmond Boyer. Articulated
715 shape matching using laplacian eigenfunctions and unsupervised point registration. In *2008 IEEE
716 Conference on Computer Vision and Pattern Recognition*, pp. 1–8. IEEE, 2008.
717
- 718 James Munkres. Algorithms for the assignment and transportation problems. *Journal of the society
719 for industrial and applied mathematics*, 5(1):32–38, 1957.
- 720 Andrea Muratori and Guilhem Semerjian. Faster algorithms for the alignment of sparse correlated
721 Erdős-Rényi random graphs. *Journal of Statistical Mechanics: Theory and Experiment*, 2024
722 (11):113405, 2024.
723
- 724 Efe Onaran, Siddharth Garg, and Elza Erkip. Optimal de-anonymization in random graphs with
725 community structure. In *2016 50th Asilomar conference on signals, systems and computers*, pp.
726 709–713. IEEE, 2016.
727
- 728 Panos M Pardalos, Franz Rendl, and Henry Wolkowicz. The quadratic assignment problem: A
729 survey and recent developments. In *Proceedings of the DIMACS Workshop on Quadratic Assign-
730 ment Problems, volume 16 of DIMACS Series in Discrete Mathematics and Theoretical Computer
731 Science*, pp. 1–42. American Mathematical Society, 1994.
- 732 Gabriel Peyré, Marco Cuturi, and Justin Solomon. Gromov-Wasserstein averaging of kernel and
733 distance matrices. In *International conference on machine learning*, pp. 2664–2672. PMLR,
734 2016.
- 735 Giovanni Piccioli, Guilhem Semerjian, Gabriele Sicuro, and Lenka Zdeborová. Aligning random
736 graphs with a sub-tree similarity message-passing algorithm. *Journal of Statistical Mechanics:
737 Theory and Experiment*, 2022(6):063401, 2022.
738
- 739 Krzysztof Polański, Matthew D Young, Zhichao Miao, Kerstin B Meyer, Sarah A Teichmann, and
740 Jong-Eun Park. BBKNN: fast batch alignment of single cell transcriptomes. *Bioinformatics*, 36
741 (3):964–965, 2020.
- 742 Yury Polyanskiy and Yihong Wu. *Information theory: From coding to learning*. Cambridge univer-
743 sity press, 2025.
744
- 745 Miklós Z Rácz and Anirudh Sridhar. Matching correlated inhomogeneous random graphs using
746 the k-core estimator. In *2023 IEEE International Symposium on Information Theory (ISIT)*, pp.
747 2499–2504. IEEE, 2023.
- 748 Flore Sentenac, Nathan Noiry, Matthieu Lerasle, Laurent Ménard, and Vianney Perchet. Online
749 matching in geometric random graphs. *Mathematics of Operations Research*, 2025.
750
- 751 Rohit Singh, Jinbo Xu, and Bonnie Berger. Global alignment of multiple protein interaction net-
752 works with application to functional orthology detection. *Proceedings of the National Academy
753 of Sciences*, 105(35):12763–12768, 2008.
754
- 755 Richard Sinkhorn. A relationship between arbitrary positive matrices and doubly stochastic matri-
ces. *The annals of mathematical statistics*, 35(2):876–879, 1964.

- 756 Yukun Song, Carey E Priebe, and Minh Tang. Independence testing for inhomogeneous random
757 graphs. *arXiv preprint arXiv:2304.09132*, 2023.
758
- 759 Patrik L Ståhl, Fredrik Salmén, Sanja Vickovic, Anna Lundmark, José Fernández Navarro, Jens
760 Magnusson, Stefania Giacomello, Michaela Asp, Jakub O Westholm, Mikael Huss, et al. Visual-
761 ization and analysis of gene expression in tissue sections by spatial transcriptomics. *Science*, 353
762 (6294):78–82, 2016.
- 763 Jianheng Tang, Weiqi Zhang, Jiajin Li, Kangfei Zhao, Fugee Tsung, and Jia Li. Robust attributed
764 graph alignment via joint structure learning and optimal transport. In *2023 IEEE 39th Interna-
765 tional Conference on Data Engineering (ICDE)*, pp. 1638–1651. IEEE, 2023.
766
- 767 Jie Tang, Jing Zhang, Limin Yao, Juanzi Li, Li Zhang, and Zhong Su. Arnetminer: extraction and
768 mining of academic social networks. In *Proceedings of the 14th ACM SIGKDD international
769 conference on Knowledge discovery and data mining*, pp. 990–998, 2008.
- 770 Vayer Titouan, Nicolas Courty, Romain Tavenard, and Rémi Flamary. Optimal transport for struc-
771 tured data with application on graphs. In *International Conference on Machine Learning*, pp.
772 6275–6284. PMLR, 2019.
- 773 Shinji Umeyama. An eigendecomposition approach to weighted graph matching problems. *IEEE
774 transactions on pattern analysis and machine intelligence*, 10(5):695–703, 1988.
775
- 776 Joshua T Vogelstein, John M Conroy, Vince Lyzinski, Louis J Podrazik, Steven G Kratzer, Eric T
777 Harley, Donniell E Fishkind, R Jacob Vogelstein, and Carey E Priebe. Fast approximate quadratic
778 programming for graph matching. *PLOS ONE*, 10(4):1–17, 2015.
- 779 Haoyu Wang, Yihong Wu, Jiaming Xu, and Israel Yolou. Random graph matching in geometric
780 models: the case of complete graphs. In *Conference on Learning Theory*, pp. 3441–3488. PMLR,
781 2022.
782
- 783 Ziao Wang, Ning Zhang, Weina Wang, and Lele Wang. On the feasible region of efficient algorithms
784 for attributed graph alignment. *IEEE Transactions on Information Theory*, 70(5):3622–3639,
785 2024.
- 786 Ziao Wang, Weina Wang, and Lele Wang. Efficient algorithms for attributed graph alignment with
787 vanishing edge correlation. *IEEE Transactions on Information Theory*, 71(6):4556–4580, 2025.
788
- 789 Patrick J Wolfe and Sofia C Olhede. Nonparametric graphon estimation. *arXiv preprint
790 arXiv:1309.5936*, 2013.
- 791 Yihong Wu, Jiaming Xu, and Sophie H Yu. Settling the sharp reconstruction thresholds of random
792 graph matching. *IEEE Transactions on Information Theory*, 68(8):5391–5417, 2022.
793
- 794 Yihong Wu, Jiaming Xu, and Sophie H Yu. Testing correlation of unlabeled random graphs. *The
795 Annals of Applied Probability*, 33(4):2519–2558, 2023.
- 796 Joonhyuk Yang and Hye Won Chung. Exact graph matching in correlated Gaussian-attributed Erdős-
797 Rényi mode. In *2024 IEEE International Symposium on Information Theory (ISIT)*, pp. 3450–
798 3455. IEEE, 2024.
- 799 Joonhyuk Yang and Hye Won Chung. Exact matching in correlated networks with node attributes for
800 improved community recovery. *IEEE Transactions on Information Theory*, 71(10):7916–7941,
801 2025.
802
- 803 Ron Zeira, Max Land, Alexander Strzalkowski, and Benjamin J Raphael. Alignment and integration
804 of spatial transcriptomics data. *Nature Methods*, 19(5):567–575, 2022.
- 805 Zhichen Zeng, Si Zhang, Yinglong Xia, and Hanghang Tong. PARROT: Position-aware regularized
806 optimal transport for network alignment. In *Proceedings of the ACM web conference 2023*, pp.
807 372–382. Association for Computing Machinery, 2023.
808
- 809 Bin Zhang and Steve Horvath. A general framework for weighted gene co-expression network
analysis. *Statistical applications in genetics and molecular biology*, 4(1), 2005.

810 Ning Zhang, Ziao Wang, Weina Wang, and Lele Wang. Attributed graph alignment. *IEEE Transactions on Information Theory*, 70(8):5910–5934, 2024.

811
812
813 Si Zhang and Hanghang Tong. Final: Fast attributed network alignment. In *Proceedings of the 22nd ACM SIGKDD international conference on knowledge discovery and data mining*, pp. 1345–1354, 2016.

814
815
816 Yuan Zhang. Consistent polynomial-time unseeded graph matching for Lipschitz graphons. *arXiv preprint arXiv:1807.11027*, 2018.

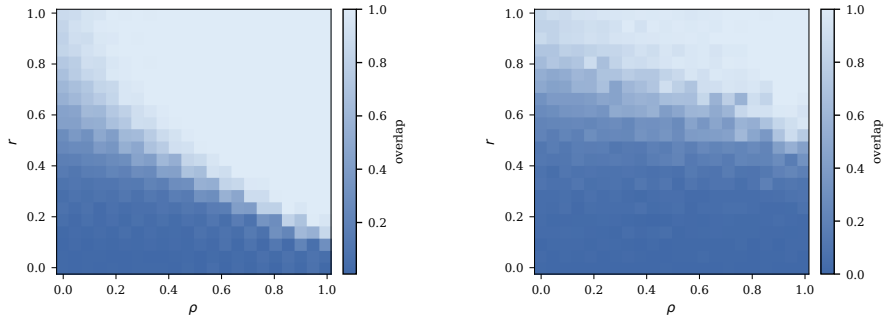
817 818 819 820 USE OF LARGE LANGUAGE MODELS (LLMs)

821
822 We acknowledge the use of Large Language Models (LLMs) solely as an auxiliary tool for polishing the language and improving the clarity of exposition. No part of the research ideation, methodology design, experimental implementation, or result analysis relied on LLMs. All technical content, proofs, and experiments were conceived, conducted, and validated entirely by the authors. The authors take full responsibility for the content of this paper.

823 824 825 826 827 A EXPERIMENTAL DETAILS

828 829 830 A.1 SYNTHETIC DATA

831
832 Figure 4 reports the results for the low-dimensional setting with $n = 100$ and $d = 16$. We again observe that the overlap increases monotonically with both ρ and r , starting near zero when both correlations vanish and approaching one when either correlation becomes large. These results mirror the high-dimensional case in Figure 1, thereby confirming that our method remains effective in both low-dimensional and high-dimensional regimes. Moreover, the numerical behavior aligns with the theoretical thresholds established in Theorem 2, while also highlighting the presence of a statistic–computation gap in certain intermediate regimes. In particular, Figure 5 illustrates how the empirical phase-transition boundaries of QPAlign, for different choices of $\lambda \in \{0.1, 0.2, \dots, 0.9\}$, closely track the information-theoretic limit, thereby providing a direct connection between the algorithm’s empirical success and our derived thresholds.



842
843
844
845
846
847
848
849
850
851
852 (a) Featured correlated Gaussian Wigner model with $n = 100$ and $d = 16$.

853
854 (b) Featured correlated Erdős-Rényi model with $n = 100$, $d = 16$, and $p = 0.5$.

855
856
857 Figure 4: Overlap between the estimator $\hat{\pi}$ in Algorithm 1 and the ground truth π^* in two models with $n = 100$ and $d = 16$, evaluated across varying correlations $\rho \in [0, 1]$ and $r \in [0, 1]$.

858
859 To facilitate a comprehensive comparison, we evaluate our approach against FGW with various fixed values of r , as well as against purely topology-based methods, including GW, Grampa, IsoRank, and Umeyama. All evaluations are conducted on synthetic featured Gaussian–Wigner graphs with $n = 100$ vertices and $d = 16$ dimensions. For the correlation parameter, we report results in terms of $\sigma = \sqrt{(1 - \rho^2)/\rho^2} \in [0, 0.5]$, which serves as a noise-to-signal ratio relative to the original graph, as showed in Figure 6. We adopt σ instead of ρ since several algorithms exhibit sharp performance transitions when $\rho \approx 1$ (i.e., $\sigma \approx 0$), making results easier to interpret under this reparametrization.

864
865
866
867
868
869
870
871
872
873
874
875
876
877
878
879
880
881
882
883
884
885
886
887
888
889
890
891
892
893
894
895
896
897
898
899
900
901
902
903
904
905
906
907
908
909
910
911
912
913
914
915
916
917

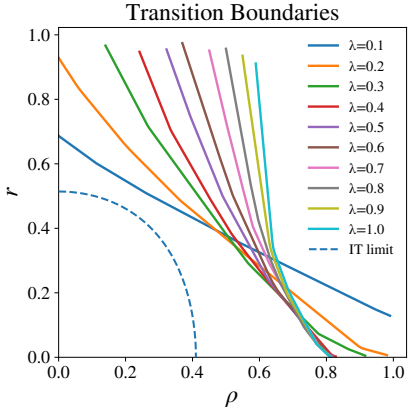


Figure 5: Phase-transition boundaries of QPAlign under different regularization parameters λ , together with the information-theoretic exact recovery limit.

In addition, we compare with FGW at fixed ρ and with MAP across different values of $r \in [0, 1]$ in Figure 7. Because MAP degenerates and becomes numerically unstable at $r = 1$, we replace the endpoint with $r = 0.999$ for all methods to ensure consistent and stable evaluation. In the synthetic data experiments presented here, our method is evaluated with step size $\eta = 10^{-4}$, $T = 400$, $K = 80$, $\lambda = 0.1$, and $\mu = 0.1$.

Figure 6 reports the alignment accuracy as a function of $\sigma = \sqrt{(1 - \rho^2)}/\rho^2$ with $\lambda = 0.05, 0.1$, and 0.15 , respectively, where smaller σ corresponds to stronger graph correlation. Our method consistently outperforms the purely edge-based baselines (GW, Grampa, IsoRank, Umeyama) and the joint edge–feature baseline FGW across different feature correlations r . Notably, even when r is small (e.g., $r = 0.1$), our approach achieves higher overlap than FGW under the same setting, indicating robustness to weak feature correlation. By contrast, classical spectral and matching-based methods (Grampa, IsoRank, Umeyama, GW) quickly degrade as noise increases.

Figure 7 shows the overlap as a function of feature correlation r with $\lambda = 0.05, 0.1$, and 0.15 , respectively, under different edge correlations ρ . Our method again demonstrates superior performance, achieving near-perfect alignment at much smaller r compared to FGW and MAP. For example, with $\rho = 0.8$, our method reaches almost perfect overlap already at $r = 0.2$, whereas FGW and MAP require significantly larger r to attain comparable accuracy. Overall, except for the degenerate case $r = 0$ or $\rho = 0$, our method consistently achieves higher overlap than existing baselines under the same r or ρ .

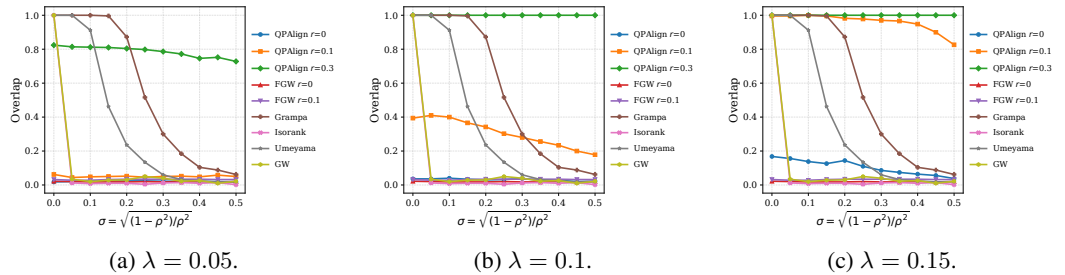


Figure 6: Overlap between the estimator $\hat{\pi}$ in Algorithm 1 and the ground truth π^* evaluated by different algorithms across varying correlations $\sigma \in [0, 0.5]$ with different λ .

To initialize for synthetic datasets, we leverage both feature and degree information to construct a mixed similarity matrix. Specifically, given node feature matrices $X = [\mathbf{x}_1^\top, \dots, \mathbf{x}_n^\top] \in \mathbb{R}^{n \times d}$ and $Y = [\mathbf{y}_1^\top, \dots, \mathbf{y}_n^\top] \in \mathbb{R}^{n \times d}$, we first compute a feature similarity matrix as $S_{\text{feat}} = \max(XY^\top, 0)$, i.e., the inner product similarity clamped elementwise at zero. We then compute a degree similarity matrix by setting $d_1 = A_1 \mathbf{1}$ and $d_2 = A_2 \mathbf{1}$, and defining $S_{\text{deg}} = (1 + |d_1 \mathbf{1}^\top - \mathbf{1} d_2^\top|)^{-1}$. These two

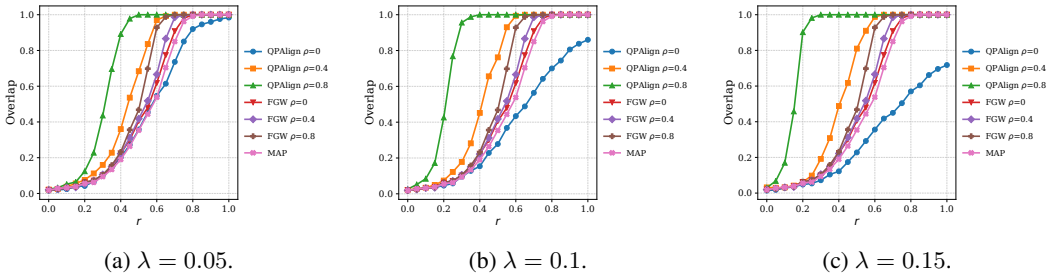


Figure 7: Overlap between the estimator $\hat{\pi}$ in Algorithm 1 and the ground truth π^* evaluated by different algorithms across varying correlations $r \in [0, 1]$ with different λ .

components are combined into a mixed similarity matrix, $S = S_{\text{feat}} + \nu S_{\text{deg}}$, which balances feature and structural signals. We empirically set $\nu = 0.1$. The initial transport plan $\Pi^{(0)}$ is then obtained by applying the Sinkhorn algorithm with K iterations to S . Across all datasets, we further employ the Barzilai–Borwein (BB) step-size rule (Barzilai & Borwein, 1988) to adaptively determine the learning rate for the gradient descent updates.

A.2 ACM-DBLP AND DOUBAN DATASETS

We introduce the construction of edges and features in the ACM-DBLP dataset as follows:

- *Features.* Features are constructed from authors and venues only, while paper titles are discarded. Author strings are lowercased, split on commas or semicolons, and tokenized by collapsing spaces into underscores. Venue names are tokenized into words, and merged phrase tokens are created. We use a pretrained RoBERTa model (Liu et al., 2021) to obtain embeddings of the corpus, and all representations are reduced to $d = 256$ dimensions via PCA before whitening to zero mean and unit variance.
- *Edges.* The graph is constructed by treating papers as nodes with edges defined by co-authorship and same-venue co-occurrence. We assign weights $\alpha = 1.0$ for shared authors and $\beta = 0.5$ for shared venues, the weight edge $\beta_{ij}(G)$ is given by

$$\tilde{\beta}_{ij}(G) = \alpha_1 C_{ij}^{\text{author}} + \alpha_2 C_{ij}^{\text{venue}}, \quad \beta_{ij}(G) = \frac{\tilde{\beta}_{ij}(G) - \mu}{\sigma},$$

where C_{ij}^{author} and C_{ij}^{venue} denote co-occurrence counts, and μ, σ are the global mean and standard deviation.

We employ the same Douban dataset used in PARROT and other prior works, without any additional processing.

Baseline comparison. For completeness, we note two method-specific adjustments. First, REGAL assumes non-negative adjacency, which does not strictly match our setting; we therefore follow the standard workaround of omitting nodes with negative degree when running REGAL. Second, PARROT is designed as an anchor-based semi-supervised method, while our experiments do not assume anchor nodes; in this case, we adopt the ablated variant without anchors described in the original paper.

For ACM-DBLP and Douban datasets, we adopt a random initialization followed by a projection step. In practice, we initialize $\Pi^{(0)}$ with a random matrix (using fixed seeds to ensure reproducibility), and then project it onto the Birkhoff polytope using the Sinkhorn algorithm. This initialization avoids numerical instabilities that may arise from directly relying on feature or degree similarities in high-dimensional sparse settings.

A.3 SPATIAL TRANSCRIPTOMIC DATA

In this subsection, we describe the experimental setup on simulated spatial transcriptomic data. Synthetic slices were generated by perturbing both spatial coordinates and transcript counts. Let

(X, Z) denote a transcript count matrix $X \in \mathbb{N}^{p \times n}$ and spot coordinates $Z \in \mathbb{R}^{2 \times n}$. To model sectioning variability, each coordinate was rotated by

$$z'_i = R(\theta)z_i, \quad R(\theta) = \begin{bmatrix} \cos \theta & -\sin \theta \\ \sin \theta & \cos \theta \end{bmatrix},$$

where θ was sampled uniformly from $[0, 2\pi)$. Spots mapped outside the array were discarded to mimic tissue loss. Pairwise distances $d_{ik} = \|z_i - z_k\|_2$ were used to ensure invariance to global translation and rotation.

Transcript counts were perturbed in two stages. First, spot-level UMI counts N_i were sampled from a negative binomial distribution $N_i \sim \text{NB}(r, p)$ with mean μ and variance σ^2 , modeling overdispersion. Second, given N_i , gene-level counts were drawn from a multinomial distribution with probabilities

$$\pi_i = \frac{x_i + \delta}{\|x_i + \delta\|_1},$$

where the pseudocount δ controls smoothing: small δ preserves heterogeneity, while large δ yields more uniform profiles. After rotation, duplicate grid positions were resolved by keeping one spot per location, preserving a one-to-one mapping. Besides, Z-score transformation was applied to both edge and feature information, and L^2 normalization was performed on the feature vectors to better align with our theoretical settings.

This perturbation procedure—combining rigid-body rotation, spot loss, and controlled count noise—produces slices that retain biological structure while reflecting realistic variability. It ensures that slices retain key biological structures while reflecting realistic experimental variability such as tissue dropout and technical noise. For example, Zeira et al. (2022) used a similar framework to study alignment robustness under geometric perturbations. We evaluated our method across different values of λ , where $\lambda = 0$ and $\lambda = 1$ correspond to feature-only and structure-only settings, respectively. The results show that our approach consistently balances edge and feature information, achieving robust performance superior to BBKNN (Polański et al., 2020) and Harmony (Korsunsky et al., 2019).

Finally, we introduce our initialization steps. We exploit domain-specific structure for initialization. Similar to synthetic datasets, we construct S_{feat} and S_{deg} , combine them with $\nu = 0.1$, and apply the Sinkhorn algorithm with K iterations to obtain $\Pi^{(0)}$.

B PROOF OF THEOREMS

B.1 PROOF OF THEOREM 1

The impossibility result directly follows from Proposition 3. We then show the possibility result. By Proposition 1,

$$\mathbb{P}[\text{d}(\hat{\pi}, \pi^*) = k] \leq \exp\left(-nh \left(\frac{k}{n}\right)\right) \mathbf{1}_{\{k \leq n-1\}} + \exp(-2 \log n) \mathbf{1}_{\{k=n\}} + \exp\left(-\frac{\epsilon k \log n}{16}\right).$$

Summing over $k \geq (1 - \delta)n$, we have

$$\begin{aligned} \sum_{k=(1-\delta)n}^{n-1} \exp\left(-nh \left(\frac{k}{n}\right)\right) &\leq \sum_{k=1}^{n-1} \exp\left(-nh \left(\frac{k}{n}\right)\right) \\ &\stackrel{(a)}{\leq} 2 \sum_{1 \leq k \leq n/2} \exp\left(-k \log \frac{n}{k}\right) \\ &\leq 2 \sum_{k=1}^{10 \log n} \exp\left(-k \log \frac{n}{k}\right) + 2 \sum_{10 \log n \leq k \leq n/2} 2^{-k} \\ &\leq 2e^{-\log n} \cdot 10 \log n + 4 \cdot 2^{-10 \log n} = n^{-1+o(1)}, \end{aligned}$$

where (a) follows from $h(x) = h(1-x)$ and $h(x) \geq x \log \frac{1}{x}$. Since

$$\sum_{k \geq (1-\delta)n} \exp\left(-\frac{1}{32}\epsilon k \log n\right) \leq \frac{\exp\left(-\frac{\epsilon}{32}(1-\delta)n \log n\right)}{1 - \exp\left(-\frac{\epsilon}{32} \log n\right)} = n^{-\Omega(n)},$$

we obtain that

$$\begin{aligned} & \sum_{k=(1-\delta)n}^n \mathbb{P}[\mathbf{d}(\hat{\pi}, \pi^*) = k] \\ & \leq \sum_{k=(1-\delta)n}^n \left[\exp\left(-nh\left(\frac{k}{n}\right)\right) \mathbf{1}_{\{k \leq n-1\}} + \exp(-2 \log n) \mathbf{1}_{\{k=n\}} + \exp\left(-\frac{\epsilon k \log n}{32}\right) \right] \\ & \leq n^{-1+o(1)} + n^{-2} + n^{-\Omega(n)}. \end{aligned} \quad (9)$$

Since $\mathbb{P}[\text{overlap}(\hat{\pi}, \pi^*) \geq \delta] \geq 1 - \sum_{k=(1-\delta)n}^n \mathbb{P}[\mathbf{d}(\hat{\pi}, \pi^*) = k]$, we finish the proof of Theorem 1.

B.2 PROOF OF THEOREM 2

The impossibility results directly follows from Proposition 4. When $n \log\left(\frac{1}{1-\rho^2}\right) + d \log\left(\frac{1}{1-r^2}\right) \geq (4+\epsilon) \log n$, we have

$$n \log\left(\frac{1}{1-\rho^2}\right) + 2d \log\left(\frac{1}{1-r^2}\right) \geq (4+\epsilon) \log n,$$

and thus equation 9 holds for $\delta = 1 - \frac{\epsilon}{16}$. It remains to upper bound $\sum_{k=1}^{\frac{\epsilon n}{16}} \mathbb{P}[\mathbf{d}(\hat{\pi}, \pi^*) = k]$. By Proposition 2,

$$\sum_{k=1}^{\frac{\epsilon n}{16}} \mathbb{P}[\mathbf{d}(\hat{\pi}, \pi^*) = k] \leq \sum_{k=1}^{\frac{\epsilon n}{16}} \exp\left(-\frac{\epsilon}{8}k \log n\right) \leq \frac{\exp(-\epsilon \log n/8)}{1 - \exp(-\epsilon \log n/8)}.$$

Combining this with equation 9, we finish the proof of Theorem 2.

B.3 PROOF OF THEOREM 3

Let $L \triangleq 2 \left\{ \lambda(\|A_1\|^2 + \|A_2\|^2)^2 + (1-\lambda) \sum_{i=1}^d (\|B_1^i\|_2 + \|B_2^i\|_2)^2 \right\}$. We first show that ∇f is L -Lipschitz. Define the linear operator

$$T(X) \triangleq \left(\sqrt{\lambda}(A_1 X - X A_2), \sqrt{1-\lambda}(B_1^1 X - X B_2^1), \dots, \sqrt{1-\lambda}(B_1^d X - X B_2^d) \right),$$

then $f(\Pi) = \|T(\Pi)\|_F^2 = \langle \Pi, T^* T \Pi \rangle$ and $\nabla f(\Pi) = 2T^* T(\Pi)$, where T^* denotes the adjoint of T with respect to the Frobenius inner product $\langle X, Y \rangle_F = \text{tr}(X^\top Y)$. Therefore,

$$\|\nabla f(X) - \nabla f(Y)\|_F \leq 2\|T\|^2 \|X - Y\|_F. \quad (10)$$

For each component of $T(X)$, $\|A_1 X - X A_2\|_F \leq (\|A_1\|_2 + \|A_2\|_2)\|X\|_F$, and similarly, $\|B_1^i X - X B_2^i\|_F \leq (\|B_1^i\|_2 + \|B_2^i\|_2)\|X\|_F$, which implies

$$\|T\|^2 \leq \lambda(\|A_1\|^2 + \|A_2\|^2)^2 + (1-\lambda) \sum_{i=1}^d (\|B_1^i\|_2 + \|B_2^i\|_2)^2.$$

Combining this with equation 10, we conclude that ∇f is L -Lipschitz.

Recall that $\Pi^{k+1} = \text{Proj}_{\mathbb{W}^n}(\Pi^k - \eta \nabla f(\Pi^k))$. Let $Y^k = \Pi^k - \eta \nabla f(\Pi^k)$. Since

$$\begin{aligned} \|X - Y^k\|_F^2 &= \|X - \Pi^k + \eta \nabla f(\Pi^k)\|_F^2 \\ &= \|X - \Pi^k\|_F^2 + 2\eta \langle \nabla f(\Pi^k), X - \Pi^k \rangle + \eta^2 \|\nabla f(\Pi^k)\|_F^2, \end{aligned}$$

we have

$$\langle \nabla f(\Pi^k), X - \Pi^k \rangle + \frac{1}{2\eta} \|X - \Pi^k\|_F^2 = \frac{1}{2\eta} \|X - Y^k\|_F^2 - \frac{\eta}{2} \|\nabla f(\Pi^k)\|_F^2.$$

Therefore, the Euclidean projection

$$\begin{aligned} \text{Proj}_{\mathbb{W}^n}(\Pi^k - \eta \nabla f(\Pi^k)) &= \arg \min_{X \in \mathbb{W}^n} \|X - Y^k\|_F^2 \\ &= \arg \min_{X \in \mathbb{W}^n} \left\{ \langle \nabla f(\Pi^k), X - \Pi^k \rangle + \frac{1}{2\eta} \|X - \Pi^k\|_F^2 \right\}. \end{aligned}$$

Since \mathbb{W}^n is convex, we have that $\Pi^{k+1} + t(\Pi - \Pi^{k+1}) \in \mathbb{W}^n$ for any $t \in (-1, 1)$ and $\Pi \in \mathbb{W}^n$.

Since Π^{k+1} minimizes $g(X) \triangleq \frac{1}{2} \|X - Y^k\|_F^2$, we have $\left. \frac{d}{dt} g(\Pi^{k+1} + t(\Pi - \Pi^{k+1})) \right|_{t=0+} \geq 0$, which implies

$$\langle \Pi^{k+1} - Y^k, \Pi - \Pi^{k+1} \rangle \geq 0 \quad (11)$$

for any $\Pi \in \mathbb{W}^n$. Consequently, take $\Pi = \Pi'$ yields that

$$\begin{aligned} \langle \nabla f(\Pi^k), \Pi^{k+1} - \Pi' \rangle &\leq \frac{1}{\eta} \langle \Pi^{k+1} - \Pi^k, \Pi^{k+1} - \Pi' \rangle \\ &= \frac{1}{2\eta} (\|\Pi^k - \Pi'\|_F^2 - \|\Pi^{k+1} - \Pi'\|_F^2 - \|\Pi^{k+1} - \Pi^k\|_F^2) \end{aligned} \quad (12)$$

We then establish the upper bound for $|f(\Pi^k) - f(\Pi')|$. For L -Lipschitz function f , we have

$$f(Y) \leq f(X) + \langle \nabla f(X), Y - X \rangle + \frac{L}{2} \|Y - X\|_F^2, \quad \forall X, Y \in \mathbb{W}^n,$$

which implies

$$f(\Pi^{k+1}) \leq f(\Pi^k) + \langle \nabla f(\Pi^k), \Pi^{k+1} - \Pi^k \rangle + \frac{L}{2} \|\Pi^{k+1} - \Pi^k\|_F^2. \quad (13)$$

We decompose the second term as

$$\langle \nabla f(\Pi^k), \Pi^{k+1} - \Pi^k \rangle = \langle \nabla f(\Pi^k), \Pi^{k+1} - \Pi' \rangle + \langle \nabla f(\Pi^k), \Pi' - \Pi^k \rangle.$$

Since f is convex, $f(\Pi') \geq f(\Pi^k) + \langle \nabla f(\Pi^k), \Pi' - \Pi^k \rangle$. Combining this with equation 12 and equation 13, we obtain that

$$\begin{aligned} f(\Pi^{k+1}) - f(\Pi') &\leq \frac{1}{2\eta} (\|\Pi^k - \Pi'\|_F^2 - \|\Pi^{k+1} - \Pi'\|_F^2 - \|\Pi^{k+1} - \Pi^k\|_F^2) + \frac{L}{2} \|\Pi^{k+1} - \Pi^k\|_F^2 \\ &= \frac{1}{2\eta} (\|\Pi^k - \Pi'\|_F^2 - \|\Pi^{k+1} - \Pi'\|_F^2) + \frac{L\eta - 1}{2\eta} \|\Pi^{k+1} - \Pi^k\|_F^2 \\ &\leq \frac{1}{2\eta} (\|\Pi^k - \Pi'\|_F^2 - \|\Pi^{k+1} - \Pi'\|_F^2), \end{aligned}$$

where the last inequality follows from $\eta \leq 1/L$.

Take $\Pi = \Pi^k$ in equation 11, we obtain that

$$\langle \nabla f(\Pi^k), \Pi^{k+1} - \Pi^k \rangle \leq -\frac{1}{\eta} \|\Pi^{k+1} - \Pi^k\|_F^2.$$

Combining this with equation 13, we obtain

$$f(\Pi^{k+1}) - f(\Pi^k) \leq \frac{L\eta - 2}{2\eta} \|\Pi^{k+1} - \Pi^k\|_F^2 \leq 0.$$

Taking sum for $k = 0, 1, \dots, K-1$, since $f(\Pi^K) \leq f(\Pi^k)$ for any $k = 0, 1, \dots, K-1$,

$$K|f(\Pi^K) - f(\Pi')| = K(f(\Pi^K) - f(\Pi')) \leq \sum_{k=0}^{K-1} f(\Pi^k) - Kf(\Pi') \leq \frac{1}{2\eta} \|\Pi^0 - \Pi'\|_F^2.$$

The Birkhoff-von Neumann theorem (see, e.g. (Horn & Johnson, 2012, Theorem 8.7.2)) states that a doubly stochastic matrix is a convex combination of permutation matrices, which implies \mathbb{W}^n is the convex hull of $n \times n$ permutation matrices. For any $P, Q \in \mathbb{W}^n$, $(P, Q) \mapsto \|P - Q\|_F^2$ is convex for each variable, hence the maximum admits on the extreme points of \mathbb{W}^n , i.e., P, Q are permutation matrices. For permutation matrices P, Q , $\text{Tr}(P^\top P) = \text{Tr}(Q^\top Q) = n$. Therefore,

$$\|\Pi^0 - \Pi'\|_F^2 \leq \|P - Q\|_F^2 = \text{Tr}(P^\top P) + \text{Tr}(Q^\top Q) - 2\text{Tr}(P^\top Q) \leq 2n.$$

Consequently,

$$|f(\Pi^K) - f(\Pi')| \leq \frac{1}{2\eta K} \|\Pi^0 - \Pi'\|_F^2 \leq \frac{n}{\eta K}.$$

C PROOF OF PROPOSITIONS

C.1 PROOF OF PROPOSITION 1

It is shown in Wu et al. (2022) and Dai et al. (2019a) that when $n \log(1/(1 - \rho^2)) \geq (4 + \epsilon) \log n$ or $d \log(1/(1 - r^2)) \geq (4 + \epsilon) \log n$ there exists an estimator $\hat{\pi}$ such that $\mathbb{P}[\hat{\pi} = \pi^*] = 1 - o(1)$. In this paper, we focus on the remaining regime, where $n \log(1/(1 - \rho^2)) \vee d \log(1/(1 - r^2)) \leq C_0 \log n$ for some universal constant $C_0 > 4$, where $a \vee b = \max(a, b)$ for any $a, b \in \mathbb{R}$. Recall that we assume $d = \omega(\log n)$, which implies that $\rho, r = o(1)$.

For any bijective mappings $\pi' : V(G_1) \mapsto V(G_2)$, let $F_{\pi'} \triangleq \{v \in V(G_1) : \pi^*(v) = \pi'(v)\}$ be the set of fixed points. Recall that $\mathcal{T}_k = \{\pi \in \mathcal{S}_n : d(\pi, \pi^*) = k\}$ and

$$\{d(\hat{\pi}, \pi^*) = k\} \subseteq \{\exists \pi' \in \mathcal{T}_k : S_{\pi^*}(G_1, G_2) \leq S_{\pi'}(G_1, G_2)\},$$

where $S_\pi(G_1, G_2) = \varphi(\rho) \sum_{e \in E(G_1)} \beta_e(G_1) \beta_{\pi(e)}(G_2) + \varphi(r) \sum_{v \in V(G_1)} \mathbf{x}_v \mathbf{y}_{\pi(v)}$. Let $G[F]$ denote the induced subgraph of G over a vertex set F . Then for any $\tau \in \mathbb{R}$, we have that

$$\begin{aligned} & \{d(\hat{\pi}, \pi^*) = k\} \\ & \subseteq \{\exists \pi' \in \mathcal{T}_k : S_{\pi^*}(G_1, G_2) \leq S_{\pi'}(G_1, G_2)\} \\ & = \{\exists \pi' \in \mathcal{T}_k : [S_{\pi^*}(G_1, G_2) - S_{\pi^*}(G_1[F_{\pi'}], G_2[F_{\pi'}])] \leq [S_{\pi'}(G_1, G_2) - S_{\pi'}(G_1[F_{\pi'}], G_2[F_{\pi'}])]\} \\ & \subseteq \{\exists \pi' \in \mathcal{T}_k : S_{\pi^*}(G_1, G_2) - S_{\pi^*}(G_1[F_{\pi'}], G_2[F_{\pi'}]) < \tau\} \\ & \quad \cup \{\exists \pi' \in \mathcal{T}_k : S_{\pi'}(G_1, G_2) - S_{\pi'}(G_1[F_{\pi'}], G_2[F_{\pi'}]) \geq \tau\}. \end{aligned}$$

We then bound the two events separately.

C.1.1 BAD EVENT OF WEAK SIGNAL

We first upper bound $\mathbb{P}[\exists \pi' \in \mathcal{T}_k : S_{\pi^*}(G_1, G_2) - S_{\pi^*}(G_1[F_{\pi'}], G_2[F_{\pi'}]) < \tau]$. We write $F = F_{\pi'}$ when π' is given. Let $N_k = \binom{n}{2} - \binom{n-k}{2}$. Without loss of generality, we define $E(G_1) \setminus \binom{F}{2} = \{e_1, e_2, \dots, e_{N_k}\}$ and $V(G_1) \setminus F = \{v_1, v_2, \dots, v_k\}$. Let $X, Y \in \mathbb{R}^{(N_k + dk) \times 1}$ be defined as

$$X \triangleq \left(\beta_{e_1}(G_1), \beta_{e_2}(G_1), \dots, \beta_{e_{N_k}}(G_1), \mathbf{x}_{v_1}^\top, \mathbf{x}_{v_2}^\top, \dots, \mathbf{x}_{v_k}^\top \right)^\top,$$

$$Y \triangleq \left(\beta_{\pi^*(e_1)}(G_2), \beta_{\pi^*(e_2)}(G_2), \dots, \beta_{\pi^*(e_{N_k})}(G_2), \mathbf{y}_{\pi^*(v_1)}^\top, \mathbf{y}_{\pi^*(v_2)}^\top, \dots, \mathbf{y}_{\pi^*(v_k)}^\top \right)^\top.$$

Let $W = S_{\pi^*}(G_1, G_2) - S_{\pi^*}(G_1[F], G_2[F])$. Then, we have that $W = X^\top A Y$, where $A = \text{diag}\{\varphi(\rho)I_{N_k}, \varphi(r)I_{dk}\}$ with $\|A\|_F^2 = \varphi(\rho)^2 N_k + \varphi(r)^2 dk$ and $\|A\|_2 = \varphi(\rho) \vee \varphi(r)$. The following Lemma provides concentration for W .

Lemma 2. *There exists a universal constant C , such that with probability at least $1 - \delta_0$,*

$$|W - (\rho\varphi(\rho)N_k + r\varphi(r)kd)| \leq C \left(\|A\|_F \sqrt{\log \frac{1}{\delta_0}} + \|A\|_2 \log \frac{1}{\delta_0} \right).$$

Pick $\tau = (\rho\varphi(\rho)N_k + r\varphi(r)kd) - a_k$, where

$$a_k = \begin{cases} 3C \sqrt{(\rho^2 N_k + r^2 kd) 2nh(\frac{k}{n})}, & k \leq n-1, \\ 3C \sqrt{(n\rho^2 + dr^2)n \log n}, & k = n, \end{cases} \quad (14)$$

and $h(x) = -x \log x - (1-x) \log(1-x)$ is the binary entropy function.

Case 1: $k = n$. We choose $\delta_0 = \exp(-2 \log n)$ in Lemma 2. Recall that $\rho, r = o(1)$. Then, with probability at least $1 - \delta_0$,

$$\begin{aligned} |W - (\rho\varphi(\rho)N_k + r\varphi(r)dk)| &\leq C \left[\sqrt{\varphi(\rho)^2 N_k + \varphi(r)^2 dk} \sqrt{2 \log n} + ((\varphi(\rho) \vee \varphi(r)) 2 \log n) \right] \\ &\leq C \sqrt{4n \log n (dr^2 + n\rho^2)} + C \sqrt{n \log n (n\rho^2 + dr^2)} \\ &= 3C \sqrt{(n\rho^2 + dr^2)n \log n} = a_n, \end{aligned}$$

where the last inequality follows from

$$(\varphi(\rho) \vee \varphi(r)) 2 \log n \leq \sqrt{n\rho^2 + dr^2} \log n \leq C \sqrt{n \log n (n\rho^2 + dr^2)}.$$

Consequently, we have $\mathbb{P}[W \leq \tau] \leq \exp(-2 \log n)$.

Case 2: $\delta n \leq k \leq n - 1$. We choose $\delta_0 = \exp(-2nh(\frac{k}{n}))$ in Lemma 2. Then, with probability $1 - \delta_0$, we have

$$\begin{aligned} &|W - (\rho\varphi(\rho)N_k + r\varphi(r)kd)| \\ &\leq C \left[\left(\sqrt{\varphi(\rho)^2 N_k + \varphi(r)^2 dk} \sqrt{2nh\left(\frac{k}{n}\right)} \right) + \left((\varphi(\rho) \vee \varphi(r)) 2nh\left(\frac{k}{n}\right) \right) \right] \\ &\leq C \left(\left(\sqrt{4(\rho^2 N_k + r^2 dk)} \sqrt{2nh\left(\frac{k}{n}\right)} \right) + \left((\varphi(\rho) \vee \varphi(r)) 2nh\left(\frac{k}{n}\right) \right) \right) \\ &\leq 3C \sqrt{(\rho^2 N_k + r^2 dk) 2nh\left(\frac{k}{n}\right)}, \end{aligned}$$

where the last inequality follows from

$$\begin{aligned} (\varphi(\rho) \vee \varphi(r)) 2nh\left(\frac{k}{n}\right) &\leq \sqrt{(\rho^2 N_k + r^2 kd) 2nh\left(\frac{k}{n}\right)} \sqrt{\frac{4n(\rho^2 + r^2)}{(\rho^2 N_k + r^2 kd)}} \\ &\leq \sqrt{(\rho^2 N_k + r^2 kd) 2nh\left(\frac{k}{n}\right)} \sqrt{\frac{8n(\rho^2 + r^2)}{k(\rho^2 n + r^2 d)}}, \end{aligned}$$

and

$$\frac{8n(\rho^2 + r^2)}{k(\rho^2 n + r^2 d)} \leq \frac{16n}{\delta n(\rho^2 n + r^2 d)} \leq \frac{16n}{\delta n(4 + \epsilon/2) \log n} \leq 1,$$

where the last inequality is because $\rho, r = o(1)$ and $n \log(\frac{1}{1-\rho^2}) + d \log(\frac{1}{1-r^2}) \geq (4 + \epsilon) \log n$ implies $n\rho^2 + dr^2 \geq (4 + \epsilon/2) \log n$. Consequently, $\mathbb{P}[W \leq \tau] \leq \exp(-2nh(\frac{k}{n}))$ when $k \leq n - 1$. By the union bound, we obtain

$$\begin{aligned} &\mathbb{P}[\exists \pi' \in \mathcal{T}_k : S_{\pi^*}(G_1, G_2) - S_{\pi^*}(G_1[F_{\pi'}], G_2[F_{\pi'}]) < \tau] \\ &\leq \mathbb{P} \left[\bigcup_{F \subseteq V(G_1): |F|=n-k} \{S_{\pi^*}(G_1, G_2) - S_{\pi^*}(G_1[F], G_2[F]) < \tau\} \right] \\ &\leq \binom{n}{k} \mathbb{P}[S_{\pi^*}(G_1, G_2) - S_{\pi^*}(G_1[F], G_2[F]) < \tau] \\ &\leq \binom{n}{k} \mathbb{P}[W \leq \tau] \mathbf{1}_{\{k \leq n-1\}} + \mathbb{P}[W \leq \tau] \mathbf{1}_{\{k=n\}} \\ &\leq \exp\left(-nh\left(\frac{k}{n}\right)\right) \mathbf{1}_{\{k \leq n-1\}} + \exp(-2 \log n) \mathbf{1}_{\{k=n\}}, \end{aligned} \tag{15}$$

where the last inequality is because $\binom{n}{k} \leq \exp(nh(\frac{k}{n}))$.

1242 C.1.2 BAD EVENT OF STRONG NOISE

1243 We then upper bound $\mathbb{P}[\exists \pi' \in \mathcal{T}_k : S_{\pi'}(G_1, G_2) - S_{\pi'}(G_1[F_{\pi'}], G_2[F_{\pi'}]) \geq \tau]$. Given π' , we define $Z \triangleq S_{\pi'}(G_1, G_2) - S_{\pi'}(G_1[F_{\pi'}], G_2[F_{\pi'}])$. We also write $F = F_{\pi'}$ when π' is given. By Chernoff's inequality, for any $t > 0$,

$$1247 \mathbb{P}[Z \geq \tau] \leq e^{-t\tau} \mathbb{E}[e^{tZ}].$$

1248 In order to compute the moment generating function $\mathbb{E}[e^{tZ}]$, we introduce the definition of orbits.

1249 **Cycle decomposition** For any $\sigma \in \mathcal{S}_n$, it induces a permutation σ^E on the edge set $(V(G_1))$ with $\sigma^E((u, v)) \triangleq (\sigma(u), \sigma(v))$ for $u, v \in V(G_1)$. We refer to σ and σ^E as a node permutation and edge permutation. Each permutation can be decomposed as disjoint cycles known as orbits. Orbits of σ (resp. σ^E) are referred as *node orbits* (resp. *edge orbits*). For example, a node orbit (u_1, u_2, \dots, u_k) indicates that $u_{i+1} = \sigma(u_i)$ for $1 \leq i \leq k-1$ and $u_1 = \sigma(u_k)$. Let n_k (resp. N_k) denote the number of k -node (resp. k -edge) orbits in σ (resp. σ^E).

1250 For any $\pi' \in \mathcal{T}_k$, let $\sigma \triangleq (\pi^*)^{-1} \circ \pi'$. Define \mathcal{C}_i^V and \mathcal{C}_i^E the set of *node orbits* and *edge orbits* of length i induced by σ , respectively. Denote $\mathcal{C}^V = \cup_{i \geq 1} \mathcal{C}_i^V$ and $\mathcal{C}^E = \cup_{i \geq 1} \mathcal{C}_i^E$. Then, $V(G_1) = \cup_{i \geq 1} \{v : v \in \mathcal{C}_i^V\}$, $E(G_1) = \cup_{i \geq 1} \{e : e \in \mathcal{C}_i^E\}$, and $\mathcal{C}_1^V = F$. Let

$$1251 Z^E = \varphi(\rho) \sum_{e \in E(G_1) \setminus (F)} \beta_e(G_1) \beta_{\pi'(e)}(G_2), \quad Z^V = \varphi(r) \sum_{v \in V(G_1) \setminus F} \mathbf{x}_v \mathbf{y}_{\pi'(v)}. \quad (16)$$

1252 Then $Z = Z^V + Z^E$. Since Z^V and Z^E are independent, we obtain that

$$1253 \mathbb{E}[e^{tZ}] = \mathbb{E}[e^{tZ^V}] \mathbb{E}[e^{tZ^E}]. \quad (17)$$

1254 We then derive the upper bounds for $\mathbb{E}[e^{tZ^V}]$ and $\mathbb{E}[e^{tZ^E}]$, respectively. For any edge cycle $C = \{e_1, e_2, \dots, e_{|C|}\}$ with $e_{i+1} = \sigma^E(e_i)$ for all $1 \leq i \leq |C| - 1$ and $e_1 = \sigma^E(e_{|C|})$, we define the cumulant generating function as

$$1255 \kappa_{|C|}^E(t) = \log \mathbb{E} \left[\exp \left(t\varphi(\rho) \sum_{i=1}^{|C|} \beta_{e_i}(G_1) \beta_{\pi'(e_i)}(G_2) \right) \right],$$

1256 where we define $(u_{|C|+1}, v_{|C|+1}) = (u_1, v_1)$. Similarly, for any node cycle $C = \{v_1, \dots, v_{|C|}\}$, we define $v_{|C|+1} = v_1$ and

$$1257 \kappa_{|C|}^V(t) = \log \mathbb{E} \left[\exp \left(t\varphi(r) \sum_{i=1}^{|C|} \mathbf{x}_{v_i} \mathbf{y}_{\pi'(v_i)} \right) \right].$$

1258 The lower-order cumulants can be calculated directly:

$$1259 \kappa_1^E(t) = -\frac{1}{2} \log(1 - 2t\rho\varphi(\rho) - t^2\varphi^2(\rho)(1 - \rho^2)),$$

$$1260 \kappa_1^V(t) = -\frac{d}{2} \log(1 - 2tr\varphi(r) - t^2\varphi^2(r)(1 - r^2)),$$

$$1261 \kappa_2^E(t) = -\frac{1}{2} \log(1 - 2t^2\varphi^2(\rho)(1 + \rho^2) + t^4\varphi^4(\rho)(1 - \rho^2)^2),$$

$$1262 \kappa_2^V(t) = -\frac{d}{2} \log(1 - 2t^2\varphi^2(r)(1 + r^2) + t^4\varphi^4(r)(1 - r^2)^2).$$

1263 Let $N_k = \binom{n}{2} - \binom{n-k}{2}$. The following Lemma provides an upper bound on the cumulant function $\log \mathbb{E}[\exp(tZ)]$.

1264 **Lemma 3.** *If $d(\pi^*, \pi') = k$, for any $0 < t \leq (\rho^{-1} - 2) \wedge (r^{-1} - 2)$, we have*

$$1265 \log \mathbb{E}[\exp(tZ)] \leq \frac{N_k}{2} \kappa_2^E(t) + \frac{k}{2} \left(\kappa_1^E(t) - \frac{1}{2} \kappa_2^E(t) + \frac{1}{2} \kappa_2^V(t) \right).$$

1296 Recall that $\tau = (\rho\varphi(\rho)N_k + r\varphi(r)kd) - a_k$, where

$$1297$$

$$1298 a_k = \begin{cases} 3C\sqrt{(\rho^2N_k + r^2kd)2nh(\frac{k}{n})}, & k \leq n-1 \\ 3C\sqrt{(n\rho^2 + dr^2)n\log n}, & k = n \end{cases} \quad (18)$$

$$1299$$

$$1300$$

1301 and $h(x) = -x\log x - (1-x)\log(1-x)$ is the binary entropy function. We then show that

$$1302$$

$$1303 \left(1 - \frac{\epsilon}{16}\right) (\rho\varphi(\rho)N_k + r\varphi(r)kd) \leq \tau \leq \rho\varphi(\rho)N_k + r\varphi(r)kd.$$

$$1304$$

1305 Recall that $\rho, r = o(1)$. For any $\delta n \leq k \leq n-1$, since $n\log\left(\frac{1}{1-\rho^2}\right) + 2d\log\left(\frac{1}{1-r^2}\right) \geq$
 1306 $(4 + \epsilon)\log n$, we have $n\rho^2 + dr^2 \geq (2 + \epsilon/4)\log n$. Therefore, we obtain $\frac{n}{k}h\left(\frac{k}{n}\right) \leq \frac{h(\delta)}{\delta} \leq$
 1307 $\frac{\epsilon^2}{2^{13}C^2}(n\rho^2 + dr^2)$ for sufficiently large n . When $k \leq n-1$, we have

$$1310 a_k = 2C\sqrt{(\rho^2N_k + r^2kd)2nh\left(\frac{k}{n}\right)} \leq 2C\sqrt{(\rho^2N_k + r^2kd)\frac{\epsilon^2}{2^{12}C^2}(n\rho^2 + dr^2)k}$$

$$1311$$

$$1312 \stackrel{(a)}{\leq} \frac{\epsilon}{32}\sqrt{(\rho^2N_k + r^2kd)4(\rho^2N_k + r^2kd)} = \frac{\epsilon}{16}(\rho^2N_k + r^2kd) \leq \frac{\epsilon}{16}(\rho\varphi(\rho)N_k + r\varphi(r)kd),$$

$$1313$$

$$1314$$

1315 where (a) is because $nk \leq 4N_k$. For $k = n$, since $n\log\left(\frac{1}{1-\rho^2}\right) + 2d\log\left(\frac{1}{1-r^2}\right) \geq (4 + \epsilon)\log n$ and
 1316 $\rho^2, r^2 = o(1)$, we conclude that $n\rho^2 + dr^2 \geq \frac{1}{2}(n\rho^2 + 2dr^2) \geq 2\log n$ holds for sufficiently large
 1317 n . Therefore,

$$1318$$

$$1319 a_k = 3C\sqrt{(n\rho^2 + dr^2)n\log n} \leq 3C\sqrt{(n\rho^2 + dr^2)\frac{(n\rho^2 + dr^2)n}{2}}$$

$$1320$$

$$1321 \leq \frac{4C}{\sqrt{n}}(\rho\varphi(\rho)n^2 + r\varphi(r)nd) \leq \frac{\epsilon}{16}(\rho\varphi(\rho)N_k + r\varphi(r)kd).$$

$$1322$$

1323 Therefore, we conclude

$$1324$$

$$1325 \left(1 - \frac{\epsilon}{16}\right) (\rho\varphi(\rho)N_k + r\varphi(r)kd) \leq \tau \leq \rho\varphi(\rho)N_k + r\varphi(r)kd.$$

$$1326$$

1327 We then upper bound $\mathbb{P}[Z \geq \tau]$. We note that

$$1328$$

$$1329 \mathbb{P}[Z \geq \tau] \leq e^{-t\tau}\mathbb{E}[e^{tZ}] \leq \exp\left(-t\tau + \frac{N_k}{2}\kappa_2^E(t) + \frac{k}{2}\left(\kappa_1^E(t) - \frac{1}{2}\kappa_2^E(t) + \frac{1}{2}\kappa_2^V(t)\right)\right).$$

$$1330$$

$$1331$$

1332 Pick $t = 1$. Since $\rho, r = o(1)$, we have $\rho^2, r^2 \leq \frac{\epsilon}{256}$. Recall that $\varphi(\rho) = \frac{\rho}{1-\rho^2}$. Then,

$$1333$$

$$1334 \kappa_1^E(t) - \frac{1}{2}\kappa_2^E(t) = \frac{1}{4}\log\frac{1 - 2t^2\varphi^2(\rho)(1 + \rho^2) + t^4\varphi^4(\rho)(1 - \rho^2)^2}{(1 - 2t\rho\varphi(\rho) - t^2\varphi^2(\rho)(1 - \rho^2))^2}$$

$$1335$$

$$1336 = \frac{1}{4}\log\left(1 + \frac{4t\rho^2}{1 - \rho^2(1 + t)^2}\right) \leq \frac{\rho^2}{1 - 4\rho^2} \leq 2,$$

$$1337$$

$$1338$$

1339 where the last inequality is because $\log(1 + x) \leq x$ and $\rho < \frac{1}{4}$. We then bound $\kappa_2^E(t)$. We note that

$$1340$$

$$1341 \frac{\kappa_2^E(t)}{\rho\varphi(\rho)} = -\frac{1 - \rho^2}{2\rho^2}\log(1 - 2t^2\varphi^2(\rho)(1 + \rho^2) + t^4\varphi^4(\rho)(1 - \rho^2)^2)$$

$$1342$$

$$1343 = -\frac{1 - \rho^2}{2\rho^2}\log\left(1 - \frac{\rho^2(2 + \rho^2)}{(1 - \rho^2)^2}\right) \stackrel{(a)}{\leq} 1 + 4\rho^2 \leq \left(1 + \frac{\epsilon}{64}\right),$$

$$1344$$

$$1345$$

1346 where the inequality (a) is from Lemma 6. Hence, we have $\kappa_2^E(t) \leq \left(1 + \frac{\epsilon}{64}\right)\rho\varphi(\rho)$. Similarly, we
 1347 have

$$1348$$

$$1349 \kappa_2^V(t) = -\frac{d}{2}\log(1 - 2t^2\varphi^2(r)(1 + r^2) + t^4\varphi^4(r)(1 - r^2)^2) \leq \left(1 + \frac{\epsilon}{64}\right)dr\varphi(r).$$

Therefore, for $t = 1$,

$$\begin{aligned}
& -t\tau + \frac{N_k}{2}\kappa_2^E(t) + \frac{k}{2}\left(\kappa_1^E(t) - \frac{1}{2}\kappa_2^E(t)\right) + \frac{k}{2}\kappa_2^V(t) \\
& \leq -\left(1 - \frac{\epsilon}{16}\right)(\rho\varphi(\rho)N_k + r\varphi(r)kd) + \left(\frac{1}{2} + \frac{\epsilon}{128}\right)(\rho\varphi(\rho)N_k + kdr\varphi(r)) + k \\
& \leq -\left(\frac{1}{2} - \frac{\epsilon}{32}\right)(\rho\varphi(\rho)N_k + r\varphi(r)kd) + k \\
& \leq -\left(\frac{1}{2} - \frac{\epsilon}{32}\right)\left(2 + \frac{\epsilon}{4}\right)k \log n + k,
\end{aligned}$$

where the last inequality is because $N_k = \binom{n}{2} - \binom{n-k}{2} \geq \frac{1}{2}\left(1 - \frac{1}{n}\right)kn$ and

$$\rho\varphi(\rho)N_k + r\varphi(r)kd \geq k\left(\frac{n-1}{2}\log\left(\frac{1}{1-\rho^2}\right) + d\log\left(\frac{1}{1-r^2}\right)\right) \geq k\left(2 + \frac{\epsilon}{4}\right)\log n.$$

Consequently, by the union bound and $|\mathcal{T}_k| = \binom{n}{k}k! \leq n^k$,

$$\begin{aligned}
& \mathbb{P}[\exists \pi' \in \mathcal{T}_k : S_{\pi'}(G_1, G_2) - S_{\pi'}(G_1[F_{\pi'}], G_2[F_{\pi'}]) \geq \tau] \\
& \leq n^k \mathbb{P}[Z \geq \tau] \\
& \leq \exp\left(k \log n - \left(\frac{1}{2} - \frac{\epsilon}{32}\right)\left(2 + \frac{\epsilon}{4}\right)k \log n + k\right) \leq \exp\left(-\frac{\epsilon}{32}k \log n\right).
\end{aligned}$$

Combining this with equation 15, we obtain that

$$\begin{aligned}
\mathbb{P}[\mathbf{d}(\hat{\pi}, \pi^*) = k] & \leq \mathbb{P}[\exists \pi' \in \mathcal{T}_k : S_{\pi^*}(G_1, G_2) - S_{\pi^*}(G_1[F_{\pi'}], G_2[F_{\pi'}]) < \tau] \\
& \quad + \mathbb{P}[\exists \pi' \in \mathcal{T}_k : S_{\pi'}(G_1, G_2) - S_{\pi'}(G_1[F_{\pi'}], G_2[F_{\pi'}]) \geq \tau] \\
& \leq \exp\left(-nh\left(\frac{k}{n}\right)\right) \mathbf{1}_{\{k \leq n-1\}} + \exp(-2 \log n) \mathbf{1}_{\{k=n\}} + \exp\left(-\frac{\epsilon k \log n}{32}\right).
\end{aligned}$$

C.2 PROOF OF PROPOSITION 2

For any $\pi' \in \mathcal{T}_k$, let

$$\begin{aligned}
Y_{\pi'} & \triangleq \varphi(\rho) \sum_{e \in E(G_1) \setminus \mathcal{C}_1^E} (\beta_e(G_1)\beta_{\pi'(e)}(G_2) - \beta_e(G_1)\beta_{\pi^*(e)}(G_2)) \\
& \quad + \varphi(r) \sum_{v \in V(G_1) \setminus \mathcal{C}_1^V} (\mathbf{x}_v^\top \mathbf{y}_{\pi'(v)} - \mathbf{x}_v^\top \mathbf{y}_{\pi^*(v)}),
\end{aligned}$$

where \mathcal{C}_1^E and \mathcal{C}_1^V denote the edge orbit and vertex orbit of length 1 induced by $\sigma = (\pi^*)^{-1} \circ \pi'$. For notational simplicity, we write $Y = Y_{\pi'}$ when π' is given. Then for any $t > 0$, $\{\mathbf{d}(\hat{\pi}, \pi^*) = k\} \subseteq \{\exists \pi' \in \mathcal{T}_k : Y \geq 0\}$ and

$$\mathbb{P}[\mathbf{d}(\hat{\pi}, \pi^*) = k] \leq \mathbb{P}[\exists \pi' \in \mathcal{T}_k : Y \geq 0] \stackrel{(a)}{\leq} |\mathcal{T}_k| \mathbb{P}[Y \geq 0] \stackrel{(b)}{\leq} n^k \mathbb{E}[\exp(tY)], \quad (19)$$

where (a) uses union bound and (b) follows from Chernoff's inequality and $|\mathcal{T}_k| = \binom{n}{k}k! \leq n^k$. Let

$$\begin{aligned}
Y^E & \triangleq \varphi(\rho) \sum_{e \in E(G_1) \setminus \mathcal{C}_1^E} (\beta_e(G_1)\beta_{\pi'(e)}(G_2) - \beta_e(G_1)\beta_{\pi^*(e)}(G_2)), \\
Y^V & \triangleq \varphi(r) \sum_{v \in V(G_1) \setminus \mathcal{C}_1^V} (\mathbf{x}_v^\top \mathbf{y}_{\pi'(v)} - \mathbf{x}_v^\top \mathbf{y}_{\pi^*(v)}).
\end{aligned}$$

Then $Y = Y^E + Y^V$ and $\mathbb{E}[\exp(tY)] = \mathbb{E}[\exp(tY^E)] \mathbb{E}[\exp(tY^V)]$. We then derive the upper bounds for $\mathbb{E}[\exp(tY^V)]$ and $\mathbb{E}[\exp(tY^E)]$, respectively. For any edge cycle $C =$

1404 $\{e_1, e_2, \dots, e_{|C|}\}$ with $e_{i+1} = \sigma^E(e_i)$ for all $1 \leq i \leq |C| - 1$ and $e_1 = \sigma^E(e_{|C|})$, we define
 1405 the cumulant generating function as

$$1406 \mu_{|C|}^E(t) = \log \mathbb{E} \left[\exp \left(t\varphi(\rho) \sum_{i=1}^{|C|} \beta_{e_i}(G_1) \beta_{\pi'(e_i)}(G_2) - t\varphi(\rho) \sum_{i=1}^{|C|} \beta_{e_i}(G_1) \beta_{\pi^*(e_i)}(G_2) \right) \right],$$

1410 where we define $(u_{|C|+1}, v_{|C|+1}) = (u_1, v_1)$. Similarly, for any node cycle $C = \{v_1, \dots, v_{|C|}\}$,
 1411 we define $v_{|C|+1} = v_1$ and

$$1412 \mu_{|C|}^V(t) = \log \mathbb{E} \left[\exp \left(t\varphi(r) \sum_{i=1}^{|C|} \mathbf{x}_{v_i} \mathbf{y}_{\pi'(v_i)} - t\varphi(r) \sum_{i=1}^{|C|} \mathbf{x}_{v_i} \mathbf{y}_{\pi^*(v_i)} \right) \right].$$

1413 The lower-order cumulants can be calculated directly:

$$1414 \mu_2^E(t) = -\frac{1}{2} \log \left(1 + \frac{\rho^2}{1 - \rho^2} (4t - 4t^2) \right), \quad \mu_2^V(t) = -\frac{d}{2} \log \left(1 + \frac{r^2}{1 - r^2} (4t - 4t^2) \right).$$

1421 Recall that $N_k = \binom{n}{2} - \binom{n-k}{2}$. The following Lemma provides an upper bound on the cumulant
 1422 function $\log \mathbb{E} [\exp(tY)]$.

1423 **Lemma 4.** *If $d(\pi^*, \pi') = k$, for any $0 < t < 1$, we have*

$$1424 \log \mathbb{E} [\exp(tY)] \leq \frac{1}{2} \left(N_k - \frac{k}{2} \right) \mu_2^E(t) + \frac{k}{2} \mu_2^V(t).$$

1425 Pick $t = \frac{1}{2}$. By Lemma 4,

$$1426 \log \mathbb{E} [\exp(tY)] \leq -\frac{nk}{4} \left(1 - \frac{k+2}{2n} \right) \log \left(\frac{1}{1 - \rho^2} \right) - \frac{kd}{4} \log \left(\frac{1}{1 - r^2} \right).$$

1427 Combining this with equation 19, we have

$$1428 \begin{aligned} \mathbb{P}[d(\hat{\pi}, \pi^*) = k] &\leq n^k \mathbb{E} [\exp(tY)] \\ &\leq \exp \left(k \log n - \frac{nk}{4} \left(1 - \frac{k+2}{2n} \right) \log \left(\frac{1}{1 - \rho^2} \right) - \frac{kd}{4} \log \left(\frac{1}{1 - r^2} \right) \right) \\ &\leq \exp \left(k \log n - \frac{k}{4} \left(1 - \frac{k+2}{2n} \right) \left(n \log \left(\frac{1}{1 - \rho^2} \right) + d \log \left(\frac{1}{1 - r^2} \right) \right) \right) \\ &\stackrel{(a)}{\leq} \exp \left(- \left(\frac{\epsilon}{4} - \frac{k+2}{2n} \left(1 + \frac{\epsilon}{4} \right) \right) k \log n \right) \stackrel{(b)}{\leq} \exp \left(-\frac{\epsilon}{8} k \log n \right), \end{aligned}$$

1433 where (a) is because $n \log \left(\frac{1}{1 - \rho^2} \right) + d \log \left(\frac{1}{1 - r^2} \right) \geq (4 + \epsilon) \log n$; (b) follows from $k \leq \frac{\epsilon}{16} n$.

1448 C.3 PROOF OF PROPOSITION 3

1449 We directly apply Fano's inequality in equation 3. For any $0 < \delta < 1$, by Lemma 1,

$$1450 \begin{aligned} \mathbb{P}[\text{overlap}(\hat{\pi}, \pi^*) < \delta] &\geq 1 - \frac{I(\pi^*; G_1, G_2) + \log 2}{\log |\mathcal{M}_\delta|} \\ &\geq 1 - \frac{\binom{n}{2} \frac{1}{2} \log \left(\frac{1}{1 - \rho^2} \right) + \frac{nd}{2} \log \left(\frac{1}{1 - r^2} \right) + \log 2}{\delta n \log(\delta n/e)} \geq 1 - \frac{c}{4\delta}, \end{aligned}$$

1451 where the last inequality follows from $n \log \left(\frac{1}{1 - \rho^2} \right) + 2d \log \left(\frac{1}{1 - r^2} \right) \leq c \log n$.

1458 C.4 PROOF OF PROPOSITION 4
1459

1460 In this subsection, we provide the proof on Proposition 4. Recall that $S_\pi(G_1, G_2) =$
1461 $\varphi(\rho) \sum_{e \in E(G_1)} \beta_e(G_1) \beta_{\pi(e)}(G_2) + \varphi(r) \sum_{v \in V(G_1)} \mathbf{x}_v \mathbf{y}_{\pi(v)}$. Define
1462

$$\begin{aligned} 1463 \mathcal{E}(\pi^*, \pi') &\triangleq \{(G_1, G_2) : S_{\pi^*}(G_1, G_2) \leq S_{\pi'}(G_1, G_2)\}, \\ 1464 \mathcal{M} &\triangleq \{\pi' \in \mathcal{S}_n : \pi' \neq \pi^*, (G_1, G_2) \in \mathcal{E}(\pi^*, \pi')\}. \end{aligned}$$

1465 Since the true permutation π^* is uniformly distributed, the MLE $\hat{\pi}_{\text{ML}}$ minimizes the error probability
1466 among all estimators. Therefore, to prove the impossibility result, it suffices to prove the failure of
1467 MLE. We note that $\hat{\pi}$ in equation 2 achieves exact recovery is equivalent to $\mathcal{M} = \emptyset$. To prove the
1468 impossibility of exact recovery, it suffices to show $\mathbb{P}[|\mathcal{M}| = 0] = o(1)$.

1469 Let $I = |\mathcal{M} \cap \mathcal{T}_2|$ with $\mathcal{T}_2 = \{\pi' \in \mathcal{S}_n : d(\pi^*, \pi') = 2\}$. Then $I \leq |\mathcal{M}|$. By Chebyshev's inequality,
1470 we have

$$1471 \mathbb{P}[|\mathcal{M}| = 0] \leq \mathbb{P}[I = 0] \leq \mathbb{P}[(I - \mathbb{E}[I])^2 \geq (\mathbb{E}[I])^2] \leq \frac{\text{Var}[I]}{(\mathbb{E}[I])^2}. \quad (20)$$

1472 Given π' , let $\epsilon_1 \triangleq \mathbb{P}[(G_1, G_2) \in \mathcal{E}(\pi^*, \pi')]$. Since $|\mathcal{T}_2| = \binom{n}{2}$, the expectation $\mathbb{E}[I]$ is then given
1473 by

$$1474 \mathbb{E}[I] = \sum_{\pi' \in \mathcal{T}_2} \mathbb{P}[(G_1, G_2) \in \mathcal{E}(\pi^*, \pi')] = \binom{n}{2} \epsilon_1.$$

1475 We then compute the second moment $\mathbb{E}[I^2]$. Note that

$$\begin{aligned} 1476 I^2 &= \left(\sum_{\pi' \in \mathcal{T}_2} \mathbf{1}_{\{(G_1, G_2) \in \mathcal{E}(\pi^*, \pi')\}} \right)^2 \\ 1477 &= \sum_{\pi' \in \mathcal{T}_2} \mathbf{1}_{\{(G_1, G_2) \in \mathcal{E}(\pi^*, \pi')\}} + \sum_{\pi_1, \pi_2 \in \mathcal{T}_2 : \pi_1 \neq \pi_2} \mathbf{1}_{\{(G_1, G_2) \in \mathcal{E}(\pi^*, \pi_1)\}} \mathbf{1}_{\{(G_1, G_2) \in \mathcal{E}(\pi^*, \pi_2)\}}. \end{aligned} \quad (21)$$

1478 It remains to compute $\sum_{\pi_1 \neq \pi_2 \in \mathcal{T}_2} \mathbb{P}[(G_1, G_2) \in \mathcal{E}(\pi^*, \pi_1) \cap \mathcal{E}(\pi^*, \pi_2)]$. Indeed, we note that
1479 $d(\pi_1, \pi_2) \in \{3, 4\}$ for $\pi_1 \neq \pi_2 \in \mathcal{T}_2$. The number of pairs (π_1, π_2) with $\pi_1 \neq \pi_2 \in \mathcal{T}_2$ with
1480 $d(\pi_1, \pi_2) = 3$ and $d(\pi_1, \pi_2) = 4$ are $6\binom{n}{3}$ and $6\binom{n}{4}$, respectively. For $\pi_1 \neq \pi_2 \in \mathcal{T}_2$ with
1481 $d(\pi_1, \pi_2) = 4$, since $S_{\pi^*}(G_1, G_2) - S_{\pi_1}(G_1, G_2)$ and $S_{\pi^*}(G_1, G_2) - S_{\pi_2}(G_1, G_2)$ are independent,
1482 we have

$$1483 \mathbb{P}[(G_1, G_2) \in \mathcal{E}(\pi^*, \pi_1) \cap \mathcal{E}(\pi^*, \pi_2)] = \mathbb{P}[(G_1, G_2) \in \mathcal{E}(\pi^*, \pi_1)] \mathbb{P}[(G_1, G_2) \in \mathcal{E}(\pi^*, \pi_2)] = \epsilon_1^2.$$

1484 For $\pi_1 \neq \pi_2 \in \mathcal{T}_2$ with $d(\pi_1, \pi_2) = 3$, we have the following Lemma.

1485 **Lemma 5.** For any $\pi_1 \neq \pi_2 \in \mathcal{T}_2$ with $d(\pi_1, \pi_2) = 3$, we have

$$1486 \mathbb{P}[(G_1, G_2) \in \mathcal{E}(\pi^*, \pi_1) \cap \mathcal{E}(\pi^*, \pi_2)] \leq (1 - \rho^2)^{\frac{3(n-2)}{4}} (1 - r^2)^{\frac{3d}{4}}.$$

Next we prove a lower bound of ϵ_1 . For any $\pi' \in \mathcal{T}_2$, we assume that $\pi^*(v) = \pi'(v)$ for any $v \in V(G_1) \setminus \{v_1, v_2\}$, $\pi^*(v_1) = \pi'(v_2)$, and $\pi^*(v_2) = \pi'(v_1)$. Consequently,

$$\begin{aligned}
\epsilon_1 &= \mathbb{P}[(G_1, G_2) \in \mathcal{E}(\pi^*, \pi')] \\
&= \mathbb{P} \left[\varphi(\rho) \sum_{e \in E(G_1)} \beta_e(G_1) (\beta_{\pi'(e)}(G_2) - \beta_{\pi^*(e)}(G_2)) \right. \\
&\quad \left. + \varphi(r) \sum_{v \in V(G_1)} \mathbf{x}_v^\top (\mathbf{y}_{\pi'(v)} - \mathbf{y}_{\pi^*(v)}) \geq 0 \right] \\
&= \mathbb{P} \left[\varphi(\rho) \sum_{v \in V(G_1) \setminus \{v_1, v_2\}} (\beta_{vv_1}(G_1) - \beta_{vv_2}(G_1)) (\beta_{\pi^*(v_1)}(G_2) - \beta_{\pi^*(v_2)}(G_2)) \right. \\
&\quad \left. + \varphi(r) (\mathbf{x}_{v_1} - \mathbf{x}_{v_2})^\top (\mathbf{y}_{\pi^*(v_1)} - \mathbf{y}_{\pi^*(v_2)}) \leq 0 \right] \\
&\geq \mathbb{P} \left[\sum_{v \in V(G_1) \setminus \{v_1, v_2\}} (\beta_{vv_1}(G_1) - \beta_{vv_2}(G_1)) (\beta_{\pi^*(v_1)}(G_2) - \beta_{\pi^*(v_2)}(G_2)) \leq 0 \right] \\
&\quad \cdot \mathbb{P} [(\mathbf{x}_{v_1} - \mathbf{x}_{v_2})^\top (\mathbf{y}_{\pi^*(v_1)} - \mathbf{y}_{\pi^*(v_2)}) \leq 0].
\end{aligned}$$

We then bound the probability of two events separately. We note that

$$\begin{bmatrix} X_v \\ Y_v \end{bmatrix} \triangleq \begin{bmatrix} \beta_{vv_1}(G_1) - \beta_{vv_2}(G_1) \\ \beta_{\pi^*(v_1)}(G_2) - \beta_{\pi^*(v_2)}(G_2) \end{bmatrix} \sim \mathcal{N} \left(\begin{bmatrix} 0 \\ 0 \end{bmatrix}, 2 \begin{bmatrix} 1 & \rho \\ \rho & 1 \end{bmatrix} \right).$$

Let $\xi_v \stackrel{\text{i.i.d.}}{\sim} \mathcal{N}(0, 1)$ for any $v \in V(G_1) \setminus \{v_1, v_2\}$. We note that

$$\begin{aligned}
&\mathbb{P} \left[\sum_{v \in V(G_1) \setminus \{v_1, v_2\}} X_v Y_v \geq 0 \right] \\
&= \mathbb{E} \left[\mathbb{P} \left[\sum_{v \in V(G_1) \setminus \{v_1, v_2\}} X_v Y_v \geq 0 \mid \{v \in V(G_1) \setminus \{v_1, v_2\}\} \right] \right] \\
&\stackrel{(a)}{=} \mathbb{E} \left[\mathbb{P} \left[\sum_{v \in V(G_1) \setminus \{v_1, v_2\}} \rho X_v^2 + 2\sqrt{1-\rho^2} X_v \xi_v \leq 0 \mid \{v \in V(G_1) \setminus \{v_1, v_2\}\} \right] \right] \\
&\stackrel{(b)}{=} \mathbb{E} \left[\mathbb{P} \left[\mathcal{N}(0, 1) \geq \frac{\rho \sqrt{\sum_{v \in V(G_1) \setminus \{v_1, v_2\}} X_v^2}}{\sqrt{2(1-\rho^2)}} \mid \{v \in V(G_1) \setminus \{v_1, v_2\}\} \right] \right],
\end{aligned}$$

where (a) is because $Y_v | X_v \sim \mathcal{N}(\rho X_v, 2(1-\rho^2))$ and $\{Y_v | X_v, v \in V(G_1) \setminus \{v_1, v_2\}\}$ are independent; (b) is because

$$\sum_{v \in V(G_1) \setminus \{v_1, v_2\}} X_v \xi_v \mid \{X_v : v \in V(G_1) \setminus \{v_1, v_2\}\} \sim \mathcal{N} \left(0, 2(1-\rho^2) \sum_{v \in V(G_1) \setminus \{v_1, v_2\}} X_v^2 \right).$$

By Lemma 7, since $\sum_{v \in V(G_1) \setminus \{v_1, v_2\}} \frac{1}{2} X_v^2 \sim \chi^2(n-2)$, we have

$$\mathbb{P} \left[\sum_{v \in V(G_1) \setminus \{v_1, v_2\}} X_v^2 \leq 2(n + \sqrt{n \log n}) \right] = 1 - o(1).$$

Consequently,

$$\begin{aligned}
& \mathbb{P} \left[\sum_{v \in V(G_1) \setminus \{v_1, v_2\}} X_v Y_v \geq 0 \right] \\
& \geq \mathbb{E} \left[(1 - o(1)) \mathbb{P} \left[\mathcal{N}(0, 1) \geq \frac{\rho \sqrt{2(n + \sqrt{n \log n})}}{\sqrt{2(1 - \rho^2)}} \right] \right] \\
& \stackrel{(a)}{\geq} \frac{1 - o(1)}{\sqrt{2\pi}} \exp \left(-\frac{1}{2} \frac{\rho^2 (n + \sqrt{n \log n})}{1 - \rho^2} \right) \frac{2}{\frac{\rho \sqrt{n + \sqrt{n \log n}}}{\sqrt{1 - \rho^2}} + \sqrt{4 + \frac{\rho^2 (n + \sqrt{n \log n})}{1 - \rho^2}}} \\
& \stackrel{(b)}{\geq} \frac{1}{16\sqrt{\log n}} (1 - \rho^2)^{-\frac{1}{2}(n-2)(1+o(1))},
\end{aligned}$$

where (a) is because $\mathbb{P}[Z \geq t] \geq \frac{2}{t + \sqrt{t^2 + 4}} \frac{1}{\sqrt{2\pi}} \exp(-\frac{1}{2}t^2)$ for $Z \sim \mathcal{N}(0, 1)$ (Birbaum, 1942);

(b) is because $n \log \left(\frac{1}{1 - \rho^2} \right) \leq (4 - \epsilon) \log n$ implies $\frac{\rho^2}{1 - \rho^2} (n + \sqrt{n \log n}) \leq 4 \log n$, $\frac{1 - o(1)}{\sqrt{2\pi}} \cdot \frac{2}{\sqrt{4 \log n + \sqrt{4 + 4 \log n}}} \geq \frac{1}{16\sqrt{\log n}}$, and $\frac{\rho^2}{1 - \rho^2} = (1 + o(1)) \log \left(\frac{1}{1 - \rho^2} \right)$. It follows from (Kunisky & Niles-Weed, 2022, Proposition 4.3) that when $r^2 \geq \frac{40}{d}$,

$$\mathbb{P}[(\mathbf{x}_{v_1} - \mathbf{x}_{v_2})^\top (\mathbf{y}_{\pi^*(v_1)} - \mathbf{y}_{\pi^*(v_2)}) \leq 0] \geq \frac{1}{1000\sqrt{d}} (1 - r^2)^{\frac{d}{2}}.$$

Consequently,

$$\epsilon_1 \geq \frac{1}{16000\sqrt{d \log n}} (1 - \rho^2)^{\frac{n-2}{2}(1+o(1))} (1 - r^2)^{\frac{d}{2}}.$$

By Lemma 5, for any $\pi_1 \neq \pi_2 \in \mathcal{T}_2$ with $d(\pi_1, \pi_2) = 3$, we have

$$\epsilon_2 \triangleq \mathbb{P}[(G_1, G_2) \in \mathcal{E}(\pi^*, \pi_1) \cap \mathcal{E}(\pi^*, \pi_2)] \leq (1 - \rho^2)^{\frac{3(n-2)}{4}} (1 - r^2)^{\frac{3d}{4}}.$$

By equation 20 and equation 21,

$$\mathbb{P}[|\mathcal{M}| = 0] \leq \frac{\mathbb{E}[I^2] - (\mathbb{E}[I])^2}{(\mathbb{E}[I])^2} = \frac{\binom{n}{2} \epsilon_1 + 6 \binom{n}{3} \epsilon_2 + 6 \binom{n}{4} \epsilon_1^2 - \binom{n}{2}^2 \epsilon_1^2}{\binom{n}{2}^2 \epsilon_1^2} \leq \frac{4}{n^2 \epsilon_1} + \frac{4\epsilon_2}{n\epsilon_1^2}.$$

Since $n \log \left(\frac{1}{1 - \rho^2} \right) + d \log \left(\frac{1}{1 - r^2} \right) + 4 \log d \leq (4 - \epsilon) \log n$, we obtain

$$\begin{aligned}
n^2 \epsilon_1 & \geq \frac{1}{16000\sqrt{\log n}} \\
& \cdot \exp \left(2 \log n - \frac{1}{2} \log d - \frac{n-2}{2} (1 + o(1)) \log \left(\frac{1}{1 - \rho^2} \right) - \frac{d}{2} \log \left(\frac{1}{1 - r^2} \right) \right) \\
& \geq \frac{1}{16000\sqrt{\log n}} \exp \left(\frac{\epsilon}{4} \log n \right)
\end{aligned}$$

and

$$\begin{aligned}
\frac{n\epsilon_1^2}{\epsilon_2} & \geq \frac{1}{256 \cdot 10^6 \log n} \\
& \cdot \exp \left(\log n - \log d - \frac{n-2}{4} (1 + o(1)) \log \left(\frac{1}{1 - \rho^2} \right) - \frac{d}{4} \log \left(\frac{1}{1 - r^2} \right) \right) \\
& \geq \frac{1}{256 \cdot 10^6 \log n} \exp \left(\frac{\epsilon}{8} \log n \right).
\end{aligned}$$

Therefore, we obtain $\mathbb{P}[|\mathcal{M}| = 0] \leq \frac{4}{n^2 \epsilon_1} + \frac{4\epsilon_2}{n\epsilon_1^2} = o(1)$, we finish the proof.

D PROOF OF LEMMAS

D.1 PROOF OF LEMMA 1

We first lower bound the packing number $|\mathcal{M}_\delta|$. For any $0 < \delta < 1$ and $\pi \in \mathcal{S}_n$, let $B(\pi, r) \triangleq \{\pi' : d(\pi, \pi') \leq r\}$ denote the ball of radius r centered at π . By a standard volume argument (Polyanskiy & Wu, 2025, Theorem 27.3), we have

$$|\mathcal{M}_\delta| \geq \frac{|\mathcal{S}_n|}{\max_\pi |B(\pi, (1-\delta)n)|} = \frac{n!}{\max_\pi |B(\pi, (1-\delta)n)|}.$$

To upper bound $|B(\pi, (1-\delta)n)|$, we first choose δn elements from the domain of π and map to the same value as π , and the remaining domain and range of size $n - \delta n$ and the mapping are selected arbitrarily. We get $|B(\pi, (1-\delta)n)| \leq \binom{n}{\delta n} (n - \delta n)!$. Consequently,

$$|\mathcal{M}_\delta| \geq \frac{n!}{\max_\pi |B(\pi, (1-\delta)n)|} \geq \frac{n!}{\binom{n}{\delta n} (n - \delta n)!} = (\delta n)! \geq \left(\frac{\delta n}{e}\right)^{\delta n}.$$

We then upper bound the mutual information. Recall that in equation 1 the likelihood function is given by

$$\mathcal{P}_{G_1, G_2 | \pi^*} = \prod_{e \in E(G_1)} P(\beta_e(G_1), \beta_{\pi^*(e)}(G_2)) \prod_{v \in V(G_1)} f(\mathbf{x}_v, \mathbf{y}_{\pi^*(v)}).$$

Next, we introduce an auxiliary distribution \mathcal{Q} under which G_1 and G_2 are independent, while maintaining the same marginals as under \mathcal{P} . Denote $Q(\cdot, \cdot)$ as the distribution of two independent standard normals and $g(\mathbf{x}, \mathbf{y})$ as the multivariate normal distribution $\mathcal{N}\left(\mathbf{0}, \begin{bmatrix} I_d & O \\ O & I_d \end{bmatrix}\right)$. Then

$$\mathcal{Q}_{G_1, G_2} = \prod_{e \in E(G_1)} Q(\beta_e(G_1), \beta_{\pi^*(e)}(G_2)) \prod_{v \in V(G_1)} g(\mathbf{x}_v, \mathbf{y}_{\pi^*(v)}).$$

The KL-divergence between the product measures $\mathcal{P}_{G_1, G_2 | \pi^*}$ and \mathcal{Q}_{G_1, G_2} is given by

$$D_{\text{KL}}(\mathcal{P}_{G_1, G_2 | \pi^*} \| \mathcal{Q}_{G_1, G_2}) = \binom{n}{2} D_{\text{KL}}(P \| Q) + n D_{\text{KL}}(f \| g).$$

We note that

$$\begin{aligned} D_{\text{KL}}(P \| Q) &= \iint P(a, b) \log \left(\frac{P(a, b)}{Q(a, b)} \right) da db \\ &= \iint P(a, b) \left[\frac{1}{2} \log \left(\frac{1}{1 - \rho^2} \right) + \frac{\rho ab}{1 - \rho^2} - \frac{\rho^2(a^2 + b^2)}{2(1 - \rho^2)} \right] da db \\ &= \frac{1}{2} \log \left(\frac{1}{1 - \rho^2} \right) + \frac{\rho^2}{1 - \rho^2} - \frac{2\rho^2}{2(1 - \rho^2)} = \frac{1}{2} \log \left(\frac{1}{1 - \rho^2} \right). \end{aligned}$$

Similarly, $D_{\text{KL}}(f \| g) = \frac{d}{2} \log \left(\frac{1}{1 - r^2} \right)$. Consequently,

$$\begin{aligned} I(\pi^*; G_1, G_2) &= \mathbb{E}_{\pi^*} [D_{\text{KL}}(\mathcal{P}_{G_1, G_2 | \pi^*} \| \mathcal{P}_{G_1, G_2})] \\ &\leq \max_{\pi \in \mathcal{S}_n} D_{\text{KL}}(\mathcal{P}_{G_1, G_2 | \pi} \| \mathcal{Q}_{G_1, G_2}) = \binom{n}{2} \frac{1}{2} \log \left(\frac{1}{1 - \rho^2} \right) + \frac{nd}{2} \log \left(\frac{1}{1 - r^2} \right). \end{aligned}$$

D.2 PROOF OF LEMMA 2

Note that $W = X^\top A Y = \frac{1}{4}(X + Y)^\top A(X + Y) - \frac{1}{4}(X - Y)^\top A(X - Y)$ and

$$\begin{aligned} \mathbb{E}[(X + Y)^\top A(X + Y)] &= (2 + 2\rho)\varphi(\rho)N_k + (2 + 2r)\varphi(r)dk \\ \mathbb{E}[(X - Y)^\top A(X - Y)] &= (2 - 2\rho)\varphi(\rho)N_k + (2 - 2r)\varphi(r)dk. \end{aligned}$$

By Hanson-Wright inequality (Hanson & Wright, 1971), there exists some universal constant C such that

$$\begin{aligned} & \mathbb{P} \left[\left| \frac{1}{4}(X+Y)^\top A(X+Y) - \mathbb{E} \left[\frac{1}{4}(X+Y)^\top A(X+Y) \right] \right| \right. \\ & \quad \left. \geq \frac{C}{2} \left(\|A\|_F \sqrt{\log \left(\frac{1}{\delta_0} \right)} \vee \|A\|_2 \log \left(\frac{1}{\delta_0} \right) \right) \right] \leq \frac{\delta_0}{2}, \\ & \mathbb{P} \left[\left| \frac{1}{4}(X-Y)^\top A(X-Y) - \mathbb{E} \left[\frac{1}{4}(X-Y)^\top A(X-Y) \right] \right| \right. \\ & \quad \left. \geq \frac{C}{2} \left(\|A\|_F \sqrt{\log \left(\frac{1}{\delta_0} \right)} \vee \|A\|_2 \log \left(\frac{1}{\delta_0} \right) \right) \right] \leq \frac{\delta_0}{2} \end{aligned}$$

for any $\delta_0 > 0$. Consequently,

$$\begin{aligned} & \mathbb{P} \left[|X^\top AY - \rho\varphi(\rho)N_k - r\varphi(r)dk| \geq C \left(\|A\|_F \sqrt{\log \left(\frac{1}{\delta_0} \right)} \vee \|A\|_2 \log \left(\frac{1}{\delta_0} \right) \right) \right] \\ & \leq \mathbb{P} \left[\left| \frac{1}{4}(X+Y)^\top A(X+Y) - \mathbb{E} \left[\frac{1}{4}(X+Y)^\top A(X+Y) \right] \right| \right. \\ & \quad \left. \geq \frac{C}{2} \left(\|A\|_F \sqrt{\log \left(\frac{1}{\delta_0} \right)} \vee \|A\|_2 \log \left(\frac{1}{\delta_0} \right) \right) \right] \\ & + \mathbb{P} \left[\left| \frac{1}{4}(X-Y)^\top A(X-Y) - \mathbb{E} \left[\frac{1}{4}(X-Y)^\top A(X-Y) \right] \right| \right. \\ & \quad \left. \geq \frac{C}{2} \left(\|A\|_F \sqrt{\log \left(\frac{1}{\delta_0} \right)} \vee \|A\|_2 \log \left(\frac{1}{\delta_0} \right) \right) \right] \leq \delta_0. \end{aligned}$$

We finish the proof of Lemma 2.

D.3 PROOF OF LEMMA 3

By equation 17, the cumulant generating function is given by

$$\log \mathbb{E} [\exp(tZ)] = \log \mathbb{E} [\exp(tZ^V)] + \log \mathbb{E} [\exp(tZ^E)].$$

We first calculate $\mathbb{E} [\exp(tZ^E)]$. Define the moment generating function (MGF) as $m_k^E = \exp(\kappa_k^E)$ for any $k \geq 1$. For any edge cycle $C = \{e_1, e_2, \dots, e_k\}$ with $e_{i+1} = \sigma^E(e_i)$ for all $1 \leq i \leq k-1$ and $e_1 = \sigma^E(e_k)$, let $A_{i-1} = \beta_{e_i}(G_1)$ and $B_i = \beta_{\pi^E(e_i)}(G_2)$ for any $1 \leq i \leq k$, and we set $A_k = A_0$ for notational simplicity. Since $\pi^*(e_{i+1}) = \pi^E(e_i)$, each pair (A_i, B_i) follows bivariate normal distribution $\mathcal{N} \left(0, \begin{bmatrix} 1 & \rho \\ \rho & 1 \end{bmatrix} \right)$, and thus the conditional distribution is given by $A_i | B_i \sim \mathcal{N}(\rho B_i, 1 - \rho^2)$. Consequently, the MGF is given by

$$\begin{aligned} m_k^E &= \mathbb{E} \left[\mathbb{E} \left[\prod_{i=1}^k \exp(t\varphi(\rho)A_{i-1}B_i) \mid B_1, \dots, B_k \right] \right] \\ &= \mathbb{E} \left[\prod_{i=1}^k \exp \left(t\rho\varphi(\rho)B_{i-1}B_i + \frac{1}{2}t^2\varphi(\rho)^2B_i^2(1-\rho^2) \right) \right], \end{aligned}$$

where the last equality is because $\mathbb{E} [\exp(tX)] = \exp(t\mu + \frac{1}{2}t^2\sigma^2)$ for $X \sim \mathcal{N}(\mu, \sigma^2)$.

Let λ_1, λ_2 denote the roots of the quadratic function $x^2 - [1 - t^2\varphi(\rho)^2(1 - \rho^2)]x + t^2\varphi(\rho)^2\rho^2 = 0$. Since $t \leq \frac{1}{\rho} - 2$, we have $\lambda_1 + \lambda_2 > 0$ and the discriminant $[1 - t^2\varphi(\rho)^2(1 - \rho^2)]^2 - 4t^2\varphi(\rho)^2\rho^2 >$

0. Since $\lambda_1 \lambda_2 > 0$, we have $\lambda_1 > \lambda_2 > 0$. Define the matrix

$$\mathbf{J}_k \triangleq \begin{bmatrix} \lambda_1^{1/2} & -\lambda_2^{1/2} & 0 & \cdots & 0 \\ 0 & \lambda_1^{1/2} & -\lambda_2^{1/2} & \cdots & 0 \\ 0 & 0 & \lambda_1^{1/2} & \cdots & 0 \\ \vdots & \vdots & \vdots & \ddots & -\lambda_2^{1/2} \\ -\lambda_2^{1/2} & 0 & \cdots & 0 & \lambda_1^{1/2} \end{bmatrix} \in \mathbb{R}^{k \times k}.$$

Denote $\mathbf{B}_k = [B_1, B_2, \dots, B_k]^\top$. Then we have

$$\begin{aligned} m_k^{\mathbb{E}} &= \mathbb{E} \left[\prod_{i=1}^k \exp \left(t \rho \varphi(\rho) B_{i-1} B_i + \frac{1}{2} t^2 \varphi(\rho)^2 B_i^2 (1 - \rho^2) \right) \right] \\ &= \int \cdots \int \left(\frac{1}{\sqrt{2\pi}} \right)^k \exp \left(-\frac{1}{2} \sum_{i=1}^k (B_i^2 - (2t\rho\varphi(\rho) B_{i-1} B_i + t^2 \varphi(\rho)^2 (1 - \rho^2) B_i^2)) \right) \\ &\quad dB_1 \cdots dB_k \\ &= \int \cdots \int \left(\frac{1}{\sqrt{2\pi}} \right)^k \exp \left(-\frac{1}{2} \sum_{i=1}^k (\lambda_1^{1/2} B_{i-1} - \lambda_2^{1/2} B_i)^2 \right) dB_1 \cdots dB_k \\ &= \int \cdots \int \left(\frac{1}{\sqrt{2\pi}} \right)^k \exp \left(-\frac{1}{2} \mathbf{B}_k^\top \mathbf{J}_k \mathbf{J}_k \mathbf{B}_k \right) dB_1 \cdots dB_k = [\det(\mathbf{J}_k)]^{-1} = \frac{1}{\lambda_1^{k/2} - \lambda_2^{k/2}}. \end{aligned}$$

We then calculate $\mathbb{E}[\exp(tZ^{\mathbb{V}})]$. Define the moment generating function (MGF) as $m_k^{\mathbb{V}} = \exp(\kappa_k^{\mathbb{V}})$ for any $k \geq 1$. For any vertex cycle $C = \{v_1, \dots, v_k\}$ with $v_{i+1} = \sigma(v_i)$ for any $1 \leq i \leq k-1$ and $v_1 = \sigma(v_k)$, let $\tilde{A}_{i-1} = \mathbf{x}_{v_i}$ and $\tilde{B}_i = \mathbf{y}_{\pi'(v_i)}$, and we set $\tilde{A}_k = \tilde{A}_0$ for notational simplicity. Since $\pi^*(v_{i+1}) = \pi'(v_i)$, each pair $(\tilde{A}_i, \tilde{B}_i) \sim \mathcal{N}(\mathbf{0}, \begin{bmatrix} I_d & rI_d \\ rI_d & I_d \end{bmatrix})$. Similarly,

$$\begin{aligned} m_k^{\mathbb{V}} &= \mathbb{E} \left[\mathbb{E} \left[\prod_{i=1}^k \exp \left(t \varphi(r) \tilde{A}_{i-1}^\top \tilde{B}_i \right) \mid \tilde{B}_1, \dots, \tilde{B}_k \right] \right] \\ &= \mathbb{E} \left[\prod_{i=1}^k \exp \left(t r \varphi(r) \tilde{B}_{i-1}^\top \tilde{B}_i + \frac{1}{2} t^2 \varphi(r)^2 \tilde{B}_i^\top \tilde{B}_i (1 - r^2) \right) \right] \\ &= \prod_{j=1}^d \mathbb{E} \left[\prod_{i=1}^k \exp \left(t r \varphi(r) \tilde{B}_{i-1,j} \tilde{B}_{i,j} + \frac{1}{2} t^2 \varphi(r)^2 \tilde{B}_{i,j} \tilde{B}_{i,j} (1 - r^2) \right) \right], \end{aligned}$$

where $\tilde{B}_{i,j}$ denotes the j -th element of vector \tilde{B}_i and the last equality is because $\tilde{B}_{i,j}$ and $\tilde{B}_{i',j'}$ are independent for any $(i, j) \neq (i', j')$. Let $\mu_1 > \mu_2$ denote two roots of the quadratic equation $x^2 - [1 - t^2 \varphi(r)^2 (1 - r^2)] x + t^2 \varphi(r)^2 r^2 = 0$. Since $t \leq \frac{1}{r} - 2$, we have $\mu_1 + \mu_2 > 0$ and the discriminant $[1 - t^2 \varphi(r)^2 (1 - r^2)]^2 - 4t^2 \varphi(r)^2 r^2 > 0$. Since $\mu_1 \mu_2 > 0$, we have $\mu_1 > \mu_2 > 0$. By a similar argument with calculation for the edge cycle, we have

$$m_k^{\mathbb{V}} = \left(\frac{1}{\mu_1^{k/2} - \mu_2^{k/2}} \right)^d.$$

For any $k \geq 2$, we have $\lambda_1^{k/2} - \lambda_2^{k/2} \geq (\lambda_1 - \lambda_2)^{k/2}$, and thus $m_k^E \leq (m_2^E)^{k/2}$ for any $k \geq 2$. Similarly, $m_k^V \leq (m_2^V)^{k/2}$ for any $k \geq 2$. Recall Z^E and Z^V defined in equation 16. We have

$$\begin{aligned}
\log \mathbb{E} [\exp(tZ)] &= \log \mathbb{E} [\exp(tZ^E)] + \log \mathbb{E} [\exp(tZ^V)] \\
&= \sum_{C \in \mathcal{C}^E \setminus \binom{F}{2}} \kappa_{|C|}^E + \sum_{C \in \mathcal{C}^V \setminus F} \kappa_{|C|}^V \\
&\stackrel{(a)}{\leq} \sum_{i \geq 2} \sum_{C \in \mathcal{C}_i^E} \frac{|C|}{2} \kappa_2^E(t) + \sum_{C \in \mathcal{C}_1^E \setminus \binom{F}{2}} \kappa_1^E(t) + \sum_{i \geq 2} \sum_{C \in \mathcal{C}_i^V} \frac{|C|}{2} \kappa_2^V(t) \\
&= \sum_{C \in \mathcal{C}^E \setminus \binom{F}{2}} \frac{|C|}{2} \kappa_2^E(t) + \sum_{C \in \mathcal{C}_1^E \setminus \binom{F}{2}} \left(\kappa_1^E(t) - \frac{1}{2} \kappa_2^E(t) \right) + \sum_{C \in \mathcal{C}^V \setminus F} \frac{|C|}{2} \kappa_2^V(t) \\
&\stackrel{(b)}{\leq} \frac{N_k}{2} \kappa_2^E(t) + \frac{k}{2} \left(\kappa_1^E - \frac{1}{2} \kappa_2^E(t) + \frac{1}{2} \kappa_2^V(t) \right),
\end{aligned}$$

where (a) is because $\kappa_k^E(t) \leq \frac{k}{2} \kappa_2^E(t)$ and $\kappa_k^V(t) \leq \frac{k}{2} \kappa_2^V(t)$ for any $k \geq 2$; (b) is because $\sum_{C \in \mathcal{C}^E \setminus \binom{F}{2}} |C| = \binom{n}{2} - \binom{n-k}{2} = N_k$, $\sum_{C \in \mathcal{C}^V \setminus F} |C| = n - (n-k) = k$. It remains to show $|\mathcal{C}_1^E \setminus \binom{F}{2}| \leq \frac{k}{2}$. Indeed, for any $e = uv \in C \in \mathcal{C}_1^E \setminus \binom{F}{2}$, we have $\pi'(uv) = \pi^*(uv)$. Since $e \notin \binom{F}{2}$, we have $\pi'(u) = \pi^*(v)$ and $\pi'(v) = \pi^*(u)$, which contribute two mismatched vertices in the reconstruction of the underlying mapping. Since the total number of mismatched vertices for $\pi \in \mathcal{T}_k$ equals k , we have $|\mathcal{C}_1^E \setminus \binom{F}{2}| \leq \frac{k}{2}$. Therefore, we finish the proof of Lemma 3.

D.4 PROOF OF LEMMA 4

The cumulant generating function is given by

$$\log \mathbb{E} [\exp(tY)] = \log \mathbb{E} [\exp(tY^V)] + \log \mathbb{E} [\exp(tY^E)].$$

We first calculate $\mathbb{E} [\exp(tY^E)]$. Define the moment generating function (MGF) as $\tilde{m}_k^E = \exp(\mu_k^E)$ for any $k \geq 1$. For any edge cycle $C = \{e_1, e_2, \dots, e_k\}$ with $e_{i+1} = \sigma^E(e_i)$ for all $1 \leq i \leq k-1$ and $e_1 = \sigma^E(e_k)$, let $A_{i-1} = \beta_{e_i}(G_1)$ and $B_i = \beta_{\pi'(e_i)}(G_2)$ for any $1 \leq i \leq k$, and we set $A_k = A_0$ for notational simplicity. Since $\pi^*(e_{i+1}) = \pi'(e_i)$, each pair (A_i, B_i) follows bivariate normal distribution $\mathcal{N}\left(0, \begin{bmatrix} 1 & \rho \\ \rho & 1 \end{bmatrix}\right)$, and thus the conditional distribution is given by $A_i | B_i \sim \mathcal{N}(\rho B_i, 1 - \rho^2)$. Consequently, the MGF is given by

$$\begin{aligned}
\tilde{m}_k^E &= \mathbb{E} \left[\mathbb{E} \left[\prod_{i=1}^k \exp(t\varphi(\rho)(A_{i-1}B_i - A_{i-1}B_{i-1})) \mid B_1, \dots, B_k \right] \right] \\
&= \mathbb{E} \left[\prod_{i=1}^k \exp \left(t\rho\varphi(\rho)B_{i-1}(B_i - B_{i-1}) + \frac{1}{2}t^2\varphi(\rho)^2(B_i - B_{i-1})^2(1 - \rho^2) \right) \right] \\
&= \mathbb{E} \left[\prod_{i=1}^k \exp \left((t\rho\varphi(\rho) - t^2\varphi(\rho)^2(1 - \rho^2))(B_{i-1}B_i - B_i^2) \right) \right],
\end{aligned}$$

where the second equality is because $\mathbb{E} [\exp(tX)] = \exp(t\mu + \frac{1}{2}t^2\sigma^2)$ for $X \sim \mathcal{N}(\mu, \sigma^2)$.

Let λ_1, λ_2 denote the roots of the quadratic function

$$x^2 - [1 - 2(t^2\varphi(\rho)^2(1 - \rho^2) - t\rho\varphi(\rho))]x + (t^2\varphi(\rho)^2(1 - \rho^2) - t\rho\varphi(\rho))^2 = 0.$$

Since $0 < t < 1$, we have

$$f(t, \rho) \triangleq t^2\varphi(\rho)^2(1 - \rho^2) - t\rho\varphi(\rho) = (t^2 - t) \frac{\rho^2}{1 - \rho^2} \in \left(-\frac{1}{4}, 0 \right).$$

Therefore, we have $\lambda_1 + \lambda_2 = 1 - 2f(t, \rho) > 0$, $\lambda_1 \lambda_2 = f(t, \rho)^2 > 0$ and the discriminant $(1 - 2f(t, \rho))^2 - 4f(t, \rho)^2 = 1 - 4f(t, \rho) > 0$, and thus $\lambda_1 > \lambda_2 > 0$. Define the matrix

$$\mathbf{J}_k \triangleq \begin{bmatrix} \lambda_1^{1/2} & -\lambda_2^{1/2} & 0 & \cdots & 0 \\ 0 & \lambda_1^{1/2} & -\lambda_2^{1/2} & \cdots & 0 \\ 0 & 0 & \lambda_1^{1/2} & \cdots & 0 \\ \vdots & \vdots & \vdots & \ddots & -\lambda_2^{1/2} \\ -\lambda_2^{1/2} & 0 & \cdots & 0 & \lambda_1^{1/2} \end{bmatrix} \in \mathbb{R}^{k \times k}.$$

Denote $\mathbf{B}_k = [B_1, B_2, \dots, B_k]^\top$. Then we have

$$\begin{aligned} \tilde{m}_k^{\mathbb{E}} &= \mathbb{E} \left[\prod_{i=1}^k \exp((t\rho\varphi(\rho) - t^2\varphi(\rho)^2(1 - \rho^2))(B_{i-1}B_i - B_i^2)) \right] \\ &= \int \cdots \int \left(\frac{1}{\sqrt{2\pi}} \right)^k \exp \left(-\frac{1}{2} \sum_{i=1}^k B_i^2 \right) \\ &\quad \exp \left(\sum_{i=1}^k [(t\rho\varphi(\rho) - t^2\varphi(\rho)^2(1 - \rho^2))(B_{i-1}B_i - B_i^2)] \right) dB_1 \cdots dB_k \\ &= \int \cdots \int \left(\frac{1}{\sqrt{2\pi}} \right)^k \exp \left(-\frac{1}{2} \sum_{i=1}^k (\lambda_1^{1/2} B_{i-1} - \lambda_2^{1/2} B_i)^2 \right) dB_1 \cdots dB_k \\ &= \int \cdots \int \left(\frac{1}{\sqrt{2\pi}} \right)^k \exp \left(-\frac{1}{2} \mathbf{B}_k^\top \mathbf{J}_k^\top \mathbf{J}_k \mathbf{B}_k \right) dB_1 \cdots dB_k \\ &= [\det(\mathbf{J}_k)]^{-1} = \frac{1}{\lambda_1^{k/2} - \lambda_2^{k/2}}. \end{aligned}$$

We then calculate $\mathbb{E}[\exp(tY^{\mathbb{V}})]$. Define the moment generating function (MGF) as $\tilde{m}_k^{\mathbb{V}} = \exp(\mu_k^{\mathbb{V}})$ for any $k \geq 1$. For any vertex cycle $C = \{v_1, \dots, v_k\}$ with $v_{i+1} = \sigma(v_i)$ for any $1 \leq i \leq k-1$ and $v_1 = \sigma(v_k)$, let $\tilde{A}_{i-1} = \mathbf{x}_{v_i}$ and $\tilde{B}_i = \mathbf{y}_{\pi'(v_i)}$, and we set $\tilde{A}_k = \tilde{A}_0$ for notational simplicity. Since $\pi^*(v_{i+1}) = \pi'(v_i)$, each pair $(\tilde{A}_i, \tilde{B}_i) \sim \mathcal{N}(\mathbf{0}, \begin{bmatrix} I_d & rI_d \\ rI_d & I_d \end{bmatrix})$. Similarly,

$$\begin{aligned} m_k^{\mathbb{V}} &= \mathbb{E} \left[\mathbb{E} \left[\prod_{i=1}^k \exp(t\varphi(r)(\tilde{A}_{i-1}^\top \tilde{B}_i - \tilde{A}_{i-1}^\top \tilde{B}_{i-1})) \mid \tilde{B}_1, \dots, \tilde{B}_k \right] \right] \\ &= \mathbb{E} \left[\prod_{i=1}^k \exp \left(tr\varphi(r)\tilde{B}_{i-1}^\top (\tilde{B}_i - \tilde{B}_{i-1}) + \frac{1}{2} t^2 \varphi(r)^2 (\tilde{B}_i - \tilde{B}_{i-1})^\top (\tilde{B}_i - \tilde{B}_{i-1})(1 - r^2) \right) \right] \\ &= \prod_{j=1}^d \mathbb{E} \left[\prod_{i=1}^k \exp((tr\varphi(r) - t^2\varphi(r)^2(1 - r^2))(B_{i-1,j}B_{i,j} - B_{i,j}^2)) \right], \end{aligned}$$

where $\tilde{B}_{i,j}$ denotes the j -th element of vector \tilde{B}_i and the last equality is because $\tilde{B}_{i,j}$ and $\tilde{B}_{i',j'}$ are independent for any $(i, j) \neq (i', j')$. Let $\mu_1 > \mu_2$ denote two roots of the quadratic equation

$$x^2 - [1 - 2(t^2\varphi(r)^2(1 - r^2) - tr\varphi(r))]x + (t^2\varphi(r)^2(1 - r^2) - tr\varphi(r))^2 = 0.$$

Since $0 < t < 1$, we have

$$f(t, r) \triangleq t^2\varphi(r)^2(1 - r^2) - tr\varphi(r) = (t^2 - t) \frac{r^2}{1 - r^2} \in \left(-\frac{1}{4}, 0 \right).$$

Therefore, we have $\lambda_1 + \lambda_2 = 1 - 2f(t, r) > 0$, $\lambda_1 \lambda_2 = f(t, r)^2 > 0$ and the discriminant $(1 - 2f(t, r))^2 - 4f(t, r)^2 = 1 - 4f(t, r) > 0$, and thus $\mu_1 > \mu_2 > 0$. By a similar argument with

1890 calculation for the edge cycle, we have
 1891

$$1892 \tilde{m}_k^V = \left(\frac{1}{\mu_1^{k/2} - \mu_2^{k/2}} \right)^d.$$

1895 For any $k \geq 2$, we have $\lambda_1^{k/2} - \lambda_2^{k/2} \geq (\lambda_1 - \lambda_2)^{k/2}$, and thus $\tilde{m}_k^E \leq (\tilde{m}_2^E)^{k/2}$ for any $k \geq 2$.
 1896 Similarly, $\tilde{m}_k^V \leq (\tilde{m}_2^V)^{k/2}$ for any $k \geq 2$.
 1897

1898 Then, we upper bound $\log \mathbb{E} [\exp(tY)]$. We have

$$1899 \begin{aligned} \log \mathbb{E} [\exp(tY)] &= \log \mathbb{E} [\exp(tY^E)] + \log \mathbb{E} [\exp(tY^V)] \\ 1900 &= \sum_{C \in \mathcal{C}^E \setminus \mathcal{C}_1^E} \mu_{|C|}^E + \sum_{C \in \mathcal{C}^V \setminus F} \mu_{|C|}^V \\ 1901 &\leq \sum_{C \in \mathcal{C}^E \setminus \mathcal{C}_1^E} \frac{|C|}{2} \mu_2^E(t) + \sum_{C \in \mathcal{C}^V \setminus F} \frac{|C|}{2} \mu_2^V(t), \end{aligned}$$

1906 where the inequality is because $\mu_k^E(t) \leq \frac{k}{2} \mu_2^E(t)$ and $\mu_k^V(t) \leq \frac{k}{2} \mu_2^V(t)$ for any $k \geq 2$. We note that

$$1908 \mu_2^E(t) = -\frac{1}{2} \log \left(1 + \frac{\rho^2}{1 - \rho^2} (4t - 4t^2) \right) < 0, \text{ for any } 0 < t < 1.$$

1910 Consequently,

$$1912 \begin{aligned} \log \mathbb{E} [\exp(tY)] &\leq \sum_{C \in \mathcal{C}^E \setminus \mathcal{C}_1^E} \frac{|C|}{2} \mu_2^E(t) + \sum_{C \in \mathcal{C}^V \setminus F} \frac{|C|}{2} \mu_2^V(t) \\ 1913 &\leq \frac{1}{2} \left(N_k - \frac{k}{2} \right) \mu_2^E(t) + \frac{k}{2} \mu_2^V(t), \end{aligned}$$

1914 where the inequality is because $\sum_{C \in \mathcal{C}^E \setminus \binom{F}{2}} |C| = \binom{n}{2} - \binom{n-k}{2} = N_k$, $\sum_{C \in \mathcal{C}^V \setminus F} |C| = n - (n - k) = k$, and $|\mathcal{C}_1^E \setminus \binom{F}{2}| \leq \frac{k}{2}$. We finish the proof of Lemma 4.
 1915
 1916
 1917

1921 D.5 PROOF OF LEMMA 5

1922 In this subsection, without loss of generality, we assume $V(G_1) = V(G_2) = [n]$. Define adjacent
 1923 matrices $A, B \in \mathbb{R}^{n \times n}$ with $A_{ij} = \beta_{ij}(G_1)$ and $B_{ij} = \beta_{ij}(G_2)$ for any $1 \leq i < j \leq n$. Let
 1924 $X, Y \in \mathbb{R}^{n \times 1}$ with $X_i = \mathbf{x}_i$ and $Y_i = \mathbf{y}_i$ with $1 \leq i \leq n$. For any $\pi \in \mathcal{S}_n$, define $A^\pi \in \mathbb{R}^{n \times n}$ with
 1925 $A_{ij}^\pi = A_{\pi(i)\pi(j)}$ for any $1 \leq i < j \leq n$, $X^\pi \in \mathbb{R}^{n \times 1}$ with $X_i^\pi = X_{\pi(i)}$ for any $1 \leq i \leq n$. For two
 1926 matrices A and B , define the inner product as $\langle A, B \rangle = \sum_{1 \leq i < j \leq n} A_{ij} B_{ij}$. Then,
 1927
 1928

$$1929 \begin{aligned} S_\pi(G_1, G_2) &= \varphi(\rho) \sum_{e \in E(G_1)} \beta_e(G_1) \beta_{\pi(e)}(G_2) + \varphi(r) \sum_{v \in V(G_1)} \mathbf{x}_v \mathbf{y}_{\pi(v)} \\ 1930 &= \varphi(\rho) \langle A, B^\pi \rangle + \varphi(r) \langle X, Y^\pi \rangle. \end{aligned}$$

1931 For any $\pi_1 \neq \pi_2 \in \mathcal{T}_2$ with $d(\pi_1, \pi_2) = 3$,

$$1932 \begin{aligned} &\mathbb{P}[(G_1, G_2) \in \mathcal{E}(\pi^*, \pi_1) \cap \mathcal{E}(\pi^*, \pi_2)] \\ 1933 &= \mathbb{E} \left[\mathbf{1}_{\{S_{\pi^*}(G_1, G_2) \leq S_{\pi_1}(G_1, G_2)\}} \mathbf{1}_{\{S_{\pi^*}(G_1, G_2) \leq S_{\pi_2}(G_1, G_2)\}} \right] \\ 1934 &\leq \mathbb{E} \left[\exp \left(\frac{1}{2} (S_{\pi_1}(G_1, G_2) - S_{\pi^*}(G_1, G_2)) \right) \exp \left(\frac{1}{2} (S_{\pi_2}(G_1, G_2) - S_{\pi^*}(G_1, G_2)) \right) \right] \\ 1935 &= \mathbb{E} \left[\exp \left(\varphi(\rho) \left(\frac{1}{2} \langle A, B^{\pi_1} \rangle + \frac{1}{2} \langle A, B^{\pi_2} \rangle - \langle A, B^{\pi^*} \rangle \right) \right) \right] \\ 1936 &\quad \cdot \mathbb{E} \left[\exp \left(\varphi(r) \left(\frac{1}{2} \langle X, Y^{\pi_1} \rangle + \frac{1}{2} \langle X, Y^{\pi_2} \rangle - \langle X, Y^{\pi^*} \rangle \right) \right) \right]. \end{aligned}$$

For simplicity, we denote $dAdB = dA_{12}dA_{13} \cdots dA_{n-1n}dB_{12}dB_{13} \cdots dB_{n-1n}$. For the first term, we note that

$$\begin{aligned} & \mathbb{E} \left[\exp \left(\varphi(\rho) \left(\frac{1}{2} \langle A, B^{\pi_1} \rangle + \frac{1}{2} \langle A, B^{\pi_2} \rangle - \langle A, B^{\pi^*} \rangle \right) \right) \right] \\ &= \left(\frac{1}{2\pi\sqrt{1-\rho^2}} \right)^{\binom{n}{2}} \\ & \quad \cdot \int \cdots \int \exp \left(\frac{\varphi(\rho)}{2} (\langle A, B^{\pi_1} \rangle + \langle A, B^{\pi_2} \rangle) - \frac{1}{2(1-\rho^2)} (\|A\|_F^2 + \|B\|_F^2) \right) dAdB. \end{aligned}$$

Let $\text{vec}(A) = (A_{12}, A_{13}, \dots, A_{21}, \dots, A_{n-1n})$ for any adjacent matrix A . For any $\pi_1 \neq \pi_2 \in \mathcal{T}_2$, define permutation matrices Π_1^E and $\Pi_2^E \in \{0, 1\}^{\binom{n}{2} \times \binom{n}{2}}$ as

$$\text{vec}(B^{\pi_1}) = \Pi_1^E \text{vec}(B), \quad \text{vec}(B^{\pi_2}) = \Pi_2^E \text{vec}(B).$$

Then,

$$\begin{aligned} & \frac{\varphi(\rho)}{2} (\langle A, B^{\pi_1} \rangle + \langle A, B^{\pi_2} \rangle) - \frac{1}{2(1-\rho^2)} (\|A\|_F^2 + \|B\|_F^2) \\ &= \frac{\rho}{2(1-\rho^2)} \text{vec}(A)^\top (\Pi_1^E + \Pi_2^E) \text{vec}(B) - \frac{1}{2(1-\rho^2)} (\|\text{vec}(A)\|_2^2 + \|\text{vec}(B)\|_2^2) \\ &= -\frac{1}{2(1-\rho^2)} \begin{bmatrix} \text{vec}(A) \\ \text{vec}(B) \end{bmatrix}^\top \Sigma \begin{bmatrix} \text{vec}(A) \\ \text{vec}(B) \end{bmatrix}, \end{aligned}$$

where $\Sigma \triangleq \begin{bmatrix} I_{\binom{n}{2} \times \binom{n}{2}} & -\frac{\rho}{2} (\Pi_1^E + \Pi_2^E) \\ -\frac{\rho}{2} (\Pi_1^E + \Pi_2^E)^\top & I_{\binom{n}{2} \times \binom{n}{2}} \end{bmatrix}$. Therefore,

$$\begin{aligned} & \mathbb{E} \left[\exp \left(\varphi(\rho) \left(\frac{1}{2} \langle A, B^{\pi_1} \rangle + \frac{1}{2} \langle A, B^{\pi_2} \rangle - \langle A, B^{\pi^*} \rangle \right) \right) \right] \\ &= \left(\frac{1}{2\pi\sqrt{1-\rho^2}} \right)^{\binom{n}{2}} \int \cdots \int \exp \left(-\frac{1}{2(1-\rho^2)} \begin{bmatrix} \text{vec}(A) \\ \text{vec}(B) \end{bmatrix}^\top \Sigma \begin{bmatrix} \text{vec}(A) \\ \text{vec}(B) \end{bmatrix} \right) dAdB \\ &= \sqrt{\frac{(1-\rho^2)^{\binom{n}{2}}}{\det(\Sigma)}}. \end{aligned}$$

Let $\sigma \triangleq \pi_2 \circ \pi_1^{-1}$. Recall that \mathcal{C}_i^E and \mathcal{C}_i^V denote the set of edge orbits and node orbits with length i induced by σ . It follows from (Dai et al., 2019a, Lemmas 4.2 and 4.3) that

$$\begin{aligned} \det(\Sigma) &= \prod_{k=1}^n \left(\prod_{j=1}^k \left(1 - \frac{\rho^2}{2} \left(1 + \cos \left(\frac{2\pi j}{k} \right) \right) \right) \right)^{|\mathcal{C}_k^E|} \\ &\geq (1-\rho^2)^{|\mathcal{C}_1^E|} \prod_{k=2}^n (1-\rho^2)^{k|\mathcal{C}_k^E|/2} = (1-\rho^2)^{\frac{1}{2}(\binom{n}{2} + |\mathcal{C}_1^E|)}, \end{aligned}$$

where the inequality follows from Lemma 8 and the last equality is because $\sum_{k=1}^n k|\mathcal{C}_k^E| = \binom{n}{2}$. Therefore,

$$\mathbb{E} \left[\exp \left(\varphi(\rho) \left(\frac{1}{2} \langle A, B^{\pi_1} \rangle + \frac{1}{2} \langle A, B^{\pi_2} \rangle - \langle A, B^{\pi^*} \rangle \right) \right) \right] \leq (1-\rho^2)^{\frac{1}{4}(\binom{n}{2} - |\mathcal{C}_1^E|)}.$$

Similarly,

$$\mathbb{E} \left[\exp \left(\varphi(r) \left(\frac{1}{2} \langle X, Y^{\pi_1} \rangle + \frac{1}{2} \langle X, Y^{\pi_2} \rangle - \langle X, Y^{\pi^*} \rangle \right) \right) \right] \leq (1-r^2)^{\frac{d(n-|\mathcal{C}_1^Y|)}{4}}.$$

For any $\pi_1 \neq \pi_2 \in \mathcal{T}_2$ with $d(\pi_1, \pi_2) = 3$. Let $F \triangleq \{i \in [n] : \pi_1(i) = \pi_2(i)\}$. Then there exists $1 \leq i, j, k \leq n$ with $i \neq j \neq k$ such that,

$$\pi_1(i) = \pi_2(j), \pi_1(j) = \pi_2(k), \pi_1(k) = \pi_2(i), \text{ and } \pi_1(\ell) = \pi_2(\ell) \text{ for any } \ell \in [n] \setminus \{i, j, k\}.$$

Then,

$$|\mathcal{C}_1^V| = |\{\ell \in [n] : \ell \notin \{i, j, k\}\}| = n - 3,$$

$$|\mathcal{C}_1^E| = |(\ell_1, \ell_2) : 1 \leq \ell_1 < \ell_2 \leq n, \ell_1, \ell_2 \notin \{i, j, k\}| = \binom{n}{2} - \binom{n-3}{2} = 3(n-2).$$

Consequently,

$$\begin{aligned} & \mathbb{P}[(G_1, G_2) \in \mathcal{E}(\pi^*, \pi_1) \cap \mathcal{E}(\pi^*, \pi_2)] \\ & \leq \mathbb{E} \left[\exp \left(\varphi(\rho) \left(\frac{1}{2} \langle A, B^{\pi_1} \rangle + \frac{1}{2} \langle A, B^{\pi_2} \rangle - \langle A, B^{\pi^*} \rangle \right) \right) \right] \\ & \quad \cdot \mathbb{E} \left[\exp \left(\varphi(r) \left(\frac{1}{2} \langle X, Y^{\pi_1} \rangle + \frac{1}{2} \langle X, Y^{\pi_2} \rangle - \langle X, Y^{\pi^*} \rangle \right) \right) \right] \\ & \leq (1 - \rho^2)^{\frac{3(n-2)}{4}} (1 - r^2)^{\frac{3d}{4}}. \end{aligned}$$

E AUXILIARY RESULTS

Lemma 6. For $0 < \rho^2 < \frac{1}{10}$, we have

$$-\frac{1 - \rho^2}{2\rho^2} \log \left(1 - \frac{\rho^2(2 + \rho^2)}{(1 - \rho^2)^2} \right) \leq 1 + 4\rho^2.$$

Proof. Let $x \triangleq \rho^2 \in (0, \frac{1}{10})$ and define

$$t \triangleq \frac{x(2+x)}{(1-x)^2}, \quad (0 < t < 1).$$

Since $x < \frac{1}{4}$, we have

$$1 - t = \frac{(1-x)^2 - x(2+x)}{(1-x)^2} = \frac{1-4x}{(1-x)^2} > 0.$$

For any $0 < t < 1$,

$$-\log(1-t) = \sum_{k=1}^{\infty} \frac{t^k}{k} = t + \sum_{k=2}^{\infty} \frac{t^k}{k} \leq t + \frac{1}{2} \sum_{k=2}^{\infty} t^k = t + \frac{t^2}{2(1-t)}.$$

Consequently, we have

$$\begin{aligned} -\frac{1-x}{2x} \log \left(1 - \frac{x(2+x)}{(1-x)^2} \right) - (1+4x) & \leq \frac{1-x}{2x} \left(t + \frac{t^2}{2(1-t)} \right) - (1+4x) \\ & = \frac{3x(-21x^2 + 20x - 2)}{4(4x^2 - 5x + 1)}. \end{aligned}$$

For $0 < x < \frac{1}{4}$, we have $4x^2 - 5x + 1 > 0$. The numerator factor $f(x) = -21x^2 + 20x - 2$ is strictly increasing on $[0, \frac{1}{10}]$ (since $f'(x) = -42x + 20 > 0$), and $f(\frac{1}{10}) = -0.21 < 0$. Thus $f(x) < 0$ for all $0 < x \leq \frac{1}{10}$, making the whole fraction nonpositive. Therefore, for any $0 < \rho^2 < \frac{1}{10}$,

$$-\frac{1 - \rho^2}{2\rho^2} \log \left(1 - \frac{\rho^2(2 + \rho^2)}{(1 - \rho^2)^2} \right) \leq 1 + 4\rho^2. \quad \square$$

Lemma 7 (Chernoff's inequality for Chi-squared distribution). Suppose ξ follows the chi-squared distribution with n degrees of freedom. Then, for any $\delta > 0$,

$$\mathbb{P}[\xi > (1 + \delta)n] \leq \exp \left(-\frac{n}{2} (\delta - \log(1 + \delta)) \right), \quad (22)$$

$$\mathbb{P}[\xi < (1 - \delta)n] \leq \exp \left(-\frac{\delta^2}{4} n \right). \quad (23)$$

2052 *Proof.* The result follows from (Ghosh, 2021, Theorems 1 and 2). □

2053 **Lemma 8.** For any integer $k \geq 1$ and any $0 \leq \rho \leq 1$, we have

$$2054 \prod_{j=1}^k \left(\left(1 - \frac{\rho^2}{2} \right) - \frac{\rho^2}{2} \cos \frac{2\pi j}{k} \right) \geq (1 - \rho^2)^{k/2}.$$

2058 *Proof.* We note that

$$2059 \left(1 - \frac{\rho^2}{2} \right) - \frac{\rho^2}{2} \cos \frac{2\pi j}{k} = 1 - \rho^2 \cos^2 \left(\frac{\pi j}{k} \right),$$

2060 so the product equals

$$2061 P = \prod_{j=1}^k \left(1 - \rho^2 \cos^2 \left(\frac{\pi j}{k} \right) \right).$$

2062 For any $a, t \in [0, 1]$, we have $1 - at \geq (1 - a)^t$, which follows from concavity of $g(t) = \ln(1 - at) - t \ln(1 - a)$ and $g(0) = g(1) = 0$. Applying this with $a = \rho^2$ and $t = \cos^2(\pi j/k)$ yields

$$2063 1 - \rho^2 \cos^2 \left(\frac{\pi j}{k} \right) \geq (1 - \rho^2)^{\cos^2(\pi j/k)}.$$

2064 Multiplying over $j = 1, \dots, k$ gives

$$2065 P \geq (1 - \rho^2)^{\sum_{j=1}^k \cos^2(\pi j/k)}.$$

2066 Since $\sum_{j=1}^k \cos^2(\pi j/k) = \sum_{j=1}^k \frac{1 + \cos(2\pi j/k)}{2} = \frac{k}{2}$, we conclude that

$$2067 P = \prod_{j=1}^k \left(\left(1 - \frac{\rho^2}{2} \right) - \frac{\rho^2}{2} \cos \frac{2\pi j}{k} \right) \geq (1 - \rho^2)^{k/2}.$$

2068 □

2081
2082
2083
2084
2085
2086
2087
2088
2089
2090
2091
2092
2093
2094
2095
2096
2097
2098
2099
2100
2101
2102
2103
2104
2105